Revised Anisotropic Site Potentials for the Water Dimer and Calculated Properties

Claude Millot, Jean-Christophe Soetens, and Marília T. C. Martins Costa

Laboratoire de Chimie Théorique, URA CNRS no. 510, Boulevard des Aiguillettes, BP 239, 54506 Vandoeuvre-lès-Nancy Cedex, France

Matthew P. Hodges and Anthony J. Stone*

University Chemical Laboratory, Lensfield Road, Cambridge CB2 1EW, U.K.

Received: August 5, 1997; In Final Form: October 27, 1997[⊗]

Two new parametrizations of a recent ab initio polarizable anisotropic site potential for water are presented. The new versions improve the description of the electrostatic interactions, add an explicit charge-transfer term, and use more accurate dispersion coefficients from the recent literature. To assess the merits of the new models, the potential energy surface of the dimer is analyzed and a comparison is made with 12 other polarizable potentials for water in the literature, most of them being currently used in computer simulation. The structure, energy, and harmonic intermolecular frequencies of the stationary points have been determined and compared with the best available ab initio calculations. The energy barriers and pathways for hydrogen atom interchange within the dimer are discussed. The second virial coefficient $B(T)$ of steam between 373 and 973 K, including first-order quantum corrections, is reported. For all the models, the quantum corrections are found to be significant at the lowest temperatures, amounting to 10−15% at 373 K. Roughly 90% of the quantum corrections arise from the rotational degrees of freedom. Among the potentials considered, only those presented in the present work and a few others are really successful in reproducing the experimental results for $B(T)$ in that temperature range.

I. Introduction

In the field of molecular statistical simulations, water is without any doubt the system for which the largest number of potential energy functions has been designed. Pairwise additive potentials, polarizable potentials, and dimer potentials supplemented by explicit three-body and four-body terms have been proposed; the water molecules may be considered as rigid, flexible, or even able to dissociate,[1,2] and the set of interacting sites can vary in number and location in the molecule (atomic, midbond, lone-pair or at arbitrary positions). Many intermolecular potentials are pairwise additive and are designed to describe as accurately as possible, within the limitations of pairwise additivity, the properties of liquid water or ice.[3−11] These potentials, which take into account the effect of polarizability in an average way, are usually only able to describe the condensed phase in a narrow range of temperature and density for which they have been adjusted and fail to reproduce the properties of the dimer and small clusters with the accuracy of quantum chemical calculations. Recent increases in computer power have allowed the routine use of more sophisticated potentials that include the molecular polarizability explicitly. Ideally, these potentials should be able to give a good description of water in all its physical states: dimer, small clusters, liquid water, and ice. Many groups have contributed to this field, and many polarizable models of water have been published.[11−29] They are built from empirical considerations, from accurate ab initio calculations on water monomer, dimer, and other small clusters, or by combining both empirical and ab initio data. These potentials have been used to simulate small clusters, liquid water, and ice and to calculate structures and thermodynamic and spectroscopic properties.

Although most intermolecular potentials for water are built empirically, much effort has gone into calibrating potentials from accurate ab initio calculations. Among the polarizable potentials NCC (Niesar−Corongiu−Clementi),[18] NCC-vib,[29] NEMO,[20,25,27] and ASP-W (anisotropic site−site potential)[24] models are recent examples. Extensive tests of the various models reveal that presently none are perfect. Even the ab initio potentials are not able to reproduce dimer, cluster, liquid water, and ice properties equally well. Although better empirical potentials can probably be designed, there is no doubt that fitting potentials on the basis of good quality quantum chemical calculations is a better strategy. As an effort to approach an accurate intermolecular potential for water, the ASP-W form was proposed.[24] As was recognized in the original paper, the global minimum of the potential energy surface (PES) of ASP-W is not exactly the linear dimer of C_s symmetry, but rather a slightly distorted structure lying 0.01 kJ/mol lower than the linear C_s dimer, which is found to be a saddle point. It is the purpose of the present work to try to improve the ASP-W model of water. We propose two new parametrizations, which are called ASP-W4 and ASP-W2 and are described in detail in section II.

To characterize the new intermolecular ASP potentials, we consider in this work the dimer properties only. In section III, the topology of the potential energy surface is examined through the location of the stationary points, and a comparison is made with the extensive ab initio calculations of Smith et al.[30] (referred to below as SSPSR) and the features of a selection of rigid-

[⊗] Abstract published in *Advance ACS Abstracts,* December 15, 1997.

S1089-5639(97)02578-4 CCC: $15.00
Published on Web 01/22/1998

molecule polarizable potentials: PSPC (polarizable simple point charge);[15] RER(pol) (reduced effective representation of liquid water interactions including polarizability);[11] POL1;[16] RPOL,[22] which we will denote by POL2 to avoid confusion with RER(pol); Sprik−Klein[14] (denoted SK below); CKL (Cieplak−Kollman−Lybrand);[17] Kozack−Jordan[23] (denoted KJ); NCC;[18] three NEMO potentials, which we call NEMO1,[19] NEMO2,[25] and NEMO3;[27] and ASP-W.[24]

In section IV, we discuss briefly the barriers and pathways to hydrogen interchange in the dimer. These processes, which are important in the interpretation of far-infrared rotation−vibration spectroscopy,[31,32] have already been investigated using quantum chemical methods.[30,33]

The second virial coefficient $B(T)$ provides a standard test of intermolecular potentials. Although it is strictly a dimer property and so does not explore any many-body effects, it nevertheless provides a useful test that must be passed by any potential that is to be used to study dimer properties. Calculations of $B(T)$ have been reported for many pair-additive effective potentials, such as RWK2 (Reimers−Watts−Klein);[9] SPC (simple point charge) and its extension SPC/E;[34] TIPS2, TIP3P, and TIP4P (transferable intermolecular potentials);[35] and empirical and ab initio dimer potentials built by Clementi's group and based on rigid[36,37] or flexible[38] molecular models. The isotopic difference in $B(T)$ between $(H_2O)_2$ and $(D_2O)_2$ has been evaluated for the BJH (Bopp−Jancsó−Heinzinger) and MCYL (Matsuoka−Clementi−Yoshimine−Lie) potentials and variants of them.[39] Calculations have also been done for polarizable models: NCC (Niesar−Corongiu−Clementi);[18] CKL (Cieplak−Kollman−Lybrand);[17] KJ;[23] ASP-W;[24] and PPC (polarizable point charge).[28] The general trend is that effective potentials, which are designed for the bulk liquid, generally give $B(T)$ values that are much more negative than experiment.[40−43] The polarizable models are usually more satisfactory. For example, NCC is quite successful and ASP-W presents a remarkable, partly fortuitous, agreement with experiment. It is also worth recalling that the empirical KJ potential has been fitted to reproduce the second virial coefficient of water. Recently, the PPC model by Kusalik et al. has also been found to reproduce $B(T)$ and the classical third virial coefficient $C(T)$ of steam much more accurately than the effective potentials TIP4P and SPC/E.[28] It is well-known that the first-order quantum corrections to $B(T)$ are positive, and their inclusion is expected to improve the agreement with the experimental determination. De Santis and Gregori[44] have estimated the quantum corrections for the pairwise additive TIP4P and MCY potentials; they found that they bring $B(T)$ close to the experimental results for MCY (Matsuoka−Clementi−Yoshimine) but leave it too negative for TIP4P. This can be understood because MCY has been fitted to ab initio calculations on the water dimer, but TIP4P is a purely effective potential adjusted to reproduce condensed-phase properties, so it is far from optimal for the dimer. The quantum corrections to $B(T)$ have also been estimated for the Stockmayer fluid, with parameters appropriate to model water;[45,46] the results indicate that the correction is roughly 10% at 343 K. MacRury and Steele[47] have computed quantum corrections for water with a model composed of a polarizable Stockmayer potential with an anisotropic term added to the Lennard-Jones interaction; they found a trend similar to that of the Stockmayer potential. We are not aware of any calculations of the first-order quantum corrections for realistic polarizable models of water. In section V, we report calculations of the second virial coefficient of steam including first-order quantum corrections for ASP-W4, ASP-W2, and a selection of models from the literature.

TABLE 1: Distributed Multipole Moments Used in the ASP-W4 Potential. See Text for Details of the Geometry. Values in Atomic Units

O at (0.0, 0.0, 0.122 992)							
Q_{00}	−0.330 960						
Q_{10}	−0.297 907						
Q_{20}	0.117 935	Q_{22c}	0.673 922				
Q_{30}	−0.151 827	Q_{32c}	0.303 856				
Q_{40}	0.114 584	Q_{42c}	−0.183 221	Q_{44c}	−0.065 424		
H_2 at (1.430 130, 0.0, −0.983 934)							
Q_{00}	0.165 480						
Q_{10}	−0.050 267	Q_{11c}	0.144 471				
Q_{20}	0.047 356	Q_{21c}	−0.085 999	Q_{22c}	0.064 345		
Q_{30}	−0.052 434	Q_{31c}	−0.117 723	Q_{32c}	0.195 233	Q_{33c}	−0.118 823
Q_{40}	−0.117 187	Q_{41c}	0.029 905	Q_{42c}	0.197 992	Q_{43c}	−0.247 286
		Q_{44c}	0.123 927				

II. Parametrization of the ASP-W4 and ASP-W2 Potentials

The ASP-W4 and ASP-W2 potentials are both modifications of the earlier potential[24] that we denote ASP-W (ASP in the original paper). In that paper another version called ASP-S was also considered, differing from ASP-W only in the dispersion energy term. ASP-W uses an accurate model of the dispersion published by Rijks and Wormer;[48] ASP-S used a simpler model proposed by Szczęśniak et al.[49] ASP-S gave worse results for the second virial coefficient than ASP-W, and we have not considered it further. In the potentials ASP-W4 and ASP-W2, the interaction energy between water molecules is expressed as the sum of electrostatic, induction, charge-transfer, dispersion, and short-range repulsion terms. They differ in that ASP-W2 is somewhat simpler in form. The molecules are assumed rigid, with an OH bond length of 0.9572 Å and an HOH angle of 104.52°. In the molecular coordinate frame, the oxygen atom is at (0, 0, 0.122 992), H_1 is at (−1.430 130, 0, −0.983 934), and H_2 is at (1.430 130, 0, −0.983 934) (all coordinates in atomic units).

For a dimer, the electrostatic energy can be written

$$E_{\mathrm{es}} = \sum_{a\in A}\sum_{b\in B} Q_t^a T_{tu}^{ab} Q_u^b \tag{1}$$

where Q_t^a and Q_u^b are spherical multipoles distributed on oxygen and hydrogen atoms (DMA analysis[50]) and T_{tu}^{ab} are interaction functions depending on the distance between sites a and b and the relative orientation of the molecules. The DMA analysis at the MP2 level used for ASP-W has been replaced by a more accurate multireference CI calculation carried out with the program MOLPRO.[51] In ASP-W4, the atomic distributed multipole expansion is truncated at the hexadecapole on each site, and the energy terms up to $1/R^5$ distance dependence (quadrupole−quadrupole, octupole−dipole, and hexadecapole−charge) are taken into account. For the potential ASP-W2, the DMA is truncated at the quadrupole on each atom and the hydrogen quadrupoles are shifted to the oxygen atom position as in the ASP-W potential. The distributed multipoles are given in Table 1. The multipoles for hydrogen H_1 are derived from those given for H_2 by $Q_{lmc}^{H_1} = (-1)^m Q_{lmc}^{H_2}$.

The dispersion energy model has the same form as in the ASP-W potential:

$$E_{\mathrm{disp}} = -\sum_{n=6}^{10}\sum_{l_1 l_2 j \kappa_1 \kappa_2} \frac{C_n(l_1,l_2,j,\kappa_1,\kappa_2)}{R^n} \bar{S}_{l_1 l_2 j}^{\kappa_1\kappa_2}(\omega_A,\omega_B,\omega)\, f_n(a,R) \tag{2}$$

where $\bar{S}_{l_1 l_2 j}^{\kappa_1\kappa_2}(\omega_A,\omega_B,\omega)$ are the normalized real components of

TABLE 2: Polarizabilities Used in the ASP-W2 and ASP-W4 Potentials, in Real Spherical Tensor Notation. Values in Atomic Units

l_1	κ_1	l_2	κ_2	$\alpha_{l_1\kappa_1 l_2\kappa_2}$
1	0	1	0	9.907
1	1*c*	1	1*c*	10.311
1	1*s*	1	1*s*	9.549
2	0	2	0	29.871
2	0	2	2*c*	−0.425
2	1*c*	2	1*c*	52.566
2	1*s*	2	1*s*	28.179
2	2*c*	2	0	−0.425
2	2*c*	2	2*c*	37.273
2	2*s*	2	2*s*	31.449
1	0	2	0	−4.249
1	0	2	2*c*	−4.409
1	1*c*	2	1*c*	−11.920
1	1*s*	2	1*s*	−3.575
2	0	1	0	−4.249
2	2*c*	1	0	−4.409
2	1*c*	1	1*c*	−11.920
2	1*s*	1	1*s*	−3.575

TABLE 3: Dispersion Parameters Used in the ASP-W2 and ASP-W4 Potentials. Values in Atomic Units

n	l_1	l_2	j	κ_1	κ_2	$C_n(l_1,l_2,j,\kappa_1,\kappa_2)$
6	0	0	0	0	0	46.4430
6	2	0	2	2*c*	0	1.8993
6	2	2	4	2*c*	2*c*	0.2486
7	1	0	1	0	0	−58.9821
7	3	0	3	0	0	10.7304
7	3	0	3	2*c*	0	−19.5368
8	0	0	0	0	0	1141.7000
8	2	0	2	0	0	31.9758
8	2	0	2	2*c*	0	85.1285
8	4	0	4	2*c*	0	46.5276
8	1	1	2	0	0	68.2097
8	1	1	0	0	0	−21.3042
8	4	0	4	0	0	−37.1667
8	3	1	4	2*c*	0	24.5168
8	3	1	4	0	0	−13.4807
8	4	0	4	4*c*	0	22.0146
8	3	3	6	2*c*	2*c*	42.4455
9	1	0	1	0	0	−1890.9954
9	3	0	3	0	0	747.0090
9	3	0	3	2*c*	0	−1465.6607
10	0	0	0	0	0	33441.0000
10	2	0	2	0	0	1015.6221
10	2	0	2	2*c*	0	1493.2275
10	4	0	4	2*c*	0	3023.1172
10	1	1	2	0	0	2642.2136
10	1	1	0	0	0	−924.9151
10	4	0	4	0	0	−2349.3333
10	3	1	4	2*c*	0	2130.9630
10	3	1	4	0	0	−1085.5140
10	4	0	4	4*c*	0	1030.4903
10	3	3	6	2*c*	2*c*	1570.9955

Stone's orientational S functions,[52] and R is the distance between the centers of mass. $f_n(a,R)$ is an incomplete gamma function of order $n+1$ (Tang−Toennies damping function). The parameter a in the damping function is equal to 1.92 au, as in ASP-W. However the dispersion coefficients $C_n(l_1,l_2,j,\kappa_1,\kappa_2)$ of ASP-W have been replaced by more recent and accurate values calculated by Wormer and Hettema.[53] From the expansion given in their paper for the C_n ($n = 6-10$), the 3, 3, 11, 3, and 11 largest contributions respectively are retained in ASP-W4 and given in Table 3. For ASP-W2, the C_8 and C_{10} expansions are further reduced to the four largest $C_n(l_1,l_2,j,\kappa_1,\kappa_2)$ coefficients.

The polarizability model is the same as for ASP-W. It includes one-site polarizabilities up to quadrupole−quadrupole, located on the oxygen atom. The values (in au) of the polarizabilities in real spherical tensor notation $\alpha_{l_1\kappa_1 l_2\kappa_2}$ are given in Table 2. Differences from ASP-W concern the iteration of the induced multipole moments to convergence for the new potentials (ASP-W used first-order induced moments) and the damping model for the induction energy. In the calculation of the induced multipole moments and of the induction energy with ASP-W, each electrostatic interaction function T_{tu}^{ab} was scaled by the square root of the damping function $f_{2l_1+2l_2+2}(a,R)$, where l_1 and l_2 are the ranks of the multipoles involved. This treatment recovers the usual Tang−Toennies damping for the dispersion, which involves the product of two interaction functions with the same distance R. However the induction interaction may involve more than one site on each molecule, so that the distance R is different for the two interaction functions involved, and this formulation then becomes rather cumbersome, especially when derivatives of the energy are needed. We have found that to a good approximation $f_n(0.725a,R) \approx [f_{2n}(a,R)]^{1/2}$, and for this reason we now use the damping function $f_{l_1+l_2+1}(0.725a,R)$ for the interaction tensors that occur in the induction energy. For ASP-W2, a for induction has been adjusted to 2.2 au, and for ASP-W4 to 1.945 au.

A charge-transfer term has been added. The charge-transfer energy has been evaluated from IMPT calculations on the dimer following a strategy proposed by one of us[54] and fitted to an atom−atom functional form similar to that of the repulsion energy, but attractive and involving only the four oxygen−hydrogen pairs for the dimer:

$$E_{\mathrm{ct}} = -K \sum_{\text{OH pairs}} \exp[-\alpha_{ab}^{\mathrm{ct}}(R_{ab} - \rho_{ab}^{\mathrm{ct}}(\Omega))] \qquad (3)$$

and

$$E_{\mathrm{rep}} = K \sum_a \sum_b \exp[-\alpha_{ab}^{\mathrm{rep}}(R_{ab} - \rho_{ab}^{\mathrm{rep}}(\Omega))] \qquad (4)$$

where R_{ab} is the distance between the atoms, and

$$\rho_{ab}(\Omega) = \sum_{l_1 l_2 j \kappa_1 \kappa_2} \bar{S}_{l_1 l_2 j}^{\kappa_1 \kappa_2}(\Omega) \rho_{l_1 l_2 j}^{\kappa_1 \kappa_2} \qquad (5)$$

K is a constant having the value 1 millihartree. The parameters $\rho_{l_1 l_2 j}^{\kappa_1 \kappa_2}$ (bohr) and α (bohr^{-1}) are given in Table 4. For pairs of identical atoms O−O and H−H, $\rho_{l_1 l_2 j}^{\kappa_1 \kappa_2} = \rho_{l_2 l_1 j}^{\kappa_2 \kappa_1}$. For the repulsion terms, the anisotropic coefficients are the same as in ASP-W, but the isotropic coefficients have been refitted. Note that the anisotropic coefficients of Table 4 are appropriate for the definition of the local axes on the hydrogen atoms of Figure 1b of ref 24, that is, with the local z axis along the OH bond and the local x axis in the molecular plane and directed away from the other H atom.

III. Stationary Points of the Water Dimer Potential Energy Surface

A. Method. For all the potentials considered, except PSPC, POL1, and POL2, the monomer geometry corresponds to the experimental equilibrium geometry of the water molecule in the gas phase: $R_{\mathrm{OH}} = 0.9572$ Å and $\theta_{\mathrm{HOH}} = 104.52°$. For the PSPC, POL1, and POL2 potentials, $R_{\mathrm{OH}} = 1.0$ Å and $\theta_{\mathrm{HOH}} = 109.47°$. For each potential, the stationary points have been located by the following procedure. Several thousand dimer configurations are generated at random, and then, for each dimer

TABLE 4: Parameters Used in the Charge-Transfer and Repulsion Terms of the ASP-W2 and ASP-W4 Potentials. Values in Atomic Units

l_1	l_2	j	κ_1	κ_2	$\rho_{l_1 l_2 j}^{\kappa_1\kappa_2}$
Charge Transfer O−H, α = 1.794 173					
0	0	0	0	0	3.899 244
0	1	1	0	0	−0.826 647
0	2	2	0	0	0.706 998
0	3	3	0	0	−0.223 902
2	0	2	2*c*	0	−0.208 578
Repulsion O−O, α = 2.002 732					
0	0	0	0	0	5.680 000
1	0	1	0	0	0.194 693
2	0	2	0	0	−0.395 620
2	0	2	2*c*	0	0.099 227
3	0	3	0	0	0.360 409
3	0	3	2*c*	0	−0.204 826
4	0	4	0	0	−0.117 409
4	0	4	2*c*	0	0.070 905
Repulsion H−H, α = 1.929 894					
0	0	0	0	0	3.880 000
0	1	1	0	0	−0.402 480
0	1	1	0	1*c*	−0.281 719
0	2	2	0	0	0.006 327
0	2	2	0	1*c*	−0.143 812
0	2	2	0	2*c*	0.032 326
0	3	3	0	0	0.068 294
0	3	3	0	1*c*	0.074 584
0	3	3	0	2*c*	0.026 826
0	3	3	0	3*c*	0.142 389
Repulsion O−H, α = 1.980 393					
0	0	0	0	0	4.780 000
1	0	1	0	0	0.194 693
2	0	2	0	0	−0.395 620
2	0	2	2*c*	0	0.099 227
3	0	3	0	0	0.360 409
3	0	3	2*c*	0	−0.204 826
4	0	4	0	0	−0.117 409
4	0	4	2*c*	0	0.070 905
0	1	1	0	0	−0.402 480
0	1	1	0	1*c*	−0.281 719
0	2	2	0	0	0.006 327
0	2	2	0	1*c*	−0.143 812
0	2	2	0	2*c*	0.032 326
0	3	3	0	0	0.068 294
0	3	3	0	1*c*	0.074 584
0	3	3	0	2*c*	0.026 826
0	3	3	0	3*c*	0.142 389

geometry, the closest stationary point was found using the subroutine C05NBF from the NAG library, or the Orient program.[55]

For each stationary point, the Hessian was calculated, either analytically, using the Orient program, or numerically. The harmonic intermolecular vibrational frequencies were then obtained by a procedure suitable for clusters composed of rigid molecular bodies first described by Pohorille et al.[56] and used by Wales and Ohmine in a study of the water clusters $(H_2O)_8$ and $(H_2O)_{20}$.[57] The atomic masses are 1.007 94 g/mol for hydrogen and 15.999 40 g/mol for oxygen. The number of imaginary intermolecular frequencies N_i is called the Hessian index of the stationary point; a minimum has index 0, and a saddle point has index 1. Higher-index stationary points are of less interest since minimum-energy pathways connecting minima cannot pass through them,[58] but they help to characterize the surface and provide a way to compare potentials.

B. General Considerations. The stationary points found for the selected intermolecular potentials are presented in Figure 1 and Tables 5−14. We believe that the most sophisticated and extensive study of the stationary points of the water dimer potential energy surface (PES) by quantum chemical calculations is the work of Smith et al.[30] (SSPSR); although there have been many more accurate studies of the global minimum, this is the only one that has explored the surface so fully. We use it as a reference, adopting the same numbering for the stationary points and extending it for new stationary points not presented in that work, but it must be borne in mind that ab initio calculations also have their limitations. In particular no corrections were made for basis set superposition error; the BSSE was estimated to be on the order of a few kJ mol^{-1}, and was different for different stationary points.

First of all, we note that the simplest empirical potentials, like PSPC and POL2, produce a PES with fewer stationary points than the 10 reported in the ab initio calculation. On the other hand, the ASP potentials have at least 14 stationary points.

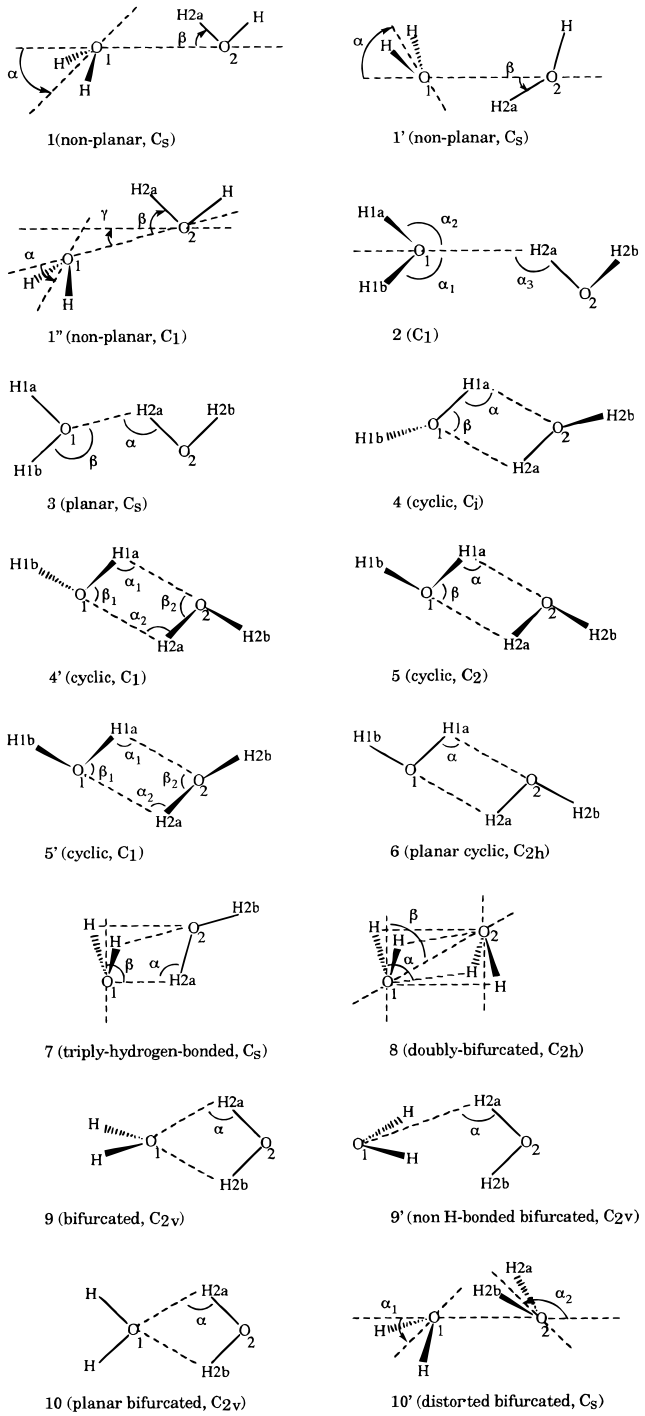

Figure 1. Stationary points of the water dimer potential energy surface.

TABLE 5: Binding Energy and Geometry of the Stationary Points (1, 1′, 1″) of the Water Dimer Potential Energy Surface Obtained from ab Initio Calculations and Various Polarizable Potentials

structure **1**	E^a	ΔE	N_i	O···O	O···H	α	β
ab initio[b]		0.000	0	2.908	1.941	45.9	2.9
ASP-W	−19.617	0.011	1	2.983	2.026	62.9	−0.1
ASP-W2	−21.072	0.000	0	2.957	2.008	64.2	6.2
ASP-W4	−20.875	0.000	0	2.970	2.014	57.0	−2.1
NEMO1	−20.783	0.000	0	2.856	1.909	72.0	6.9
NEMO2	−19.722	0.000	0	2.876	1.923	59.1	4.4
NEMO3	−20.118	0.000	0	2.901	1.953	63.6	6.5
NCC	−21.331	0.000	0	2.963	2.006	27.3	−0.3
CKL	−23.199	0.000	0	2.944	1.992	75.0	4.5
SK	−19.015	0.000	0	2.827	1.870	45.4	0.2
POL1	−23.526	0.000	0	2.754	1.756	20.7	−2.5
POL2	−22.886	0.000	0	2.786	1.788	19.7	−2.6
KJ	−21.544	0.000	0	2.981	2.028	62.4	4.4
PSPC	−18.010	0.000	0	2.855	1.857	19.3	−3.1
RER(pol)	−14.644	0.000	0	2.945	1.991	18.4	−5.3

structure **1′**	E	ΔE	N_i	O···O	O···H	α	β
ASP-W a	−17.211	2.417	1	2.998	2.057	55.8	8.7
ASP-W b	−16.311	3.317	1	3.050	2.110	12.8	9.0
ASP-W2 a	−17.957	3.115	1	2.992	2.042	52.2	5.5
ASP-W2 b	−16.968	4.104	1	3.049	2.102	12.8	7.1
ASP-W4	−17.906	2.969	1	3.000	2.049	49.8	5.1

structure **1″**	E	ΔE	N_i	O···O	O···H	α	β	γ
ASP-W	−19.628	0.000	0	2.972	2.0028	64.6	−7.8	11.5

[a] E (kJ mol^{-1}) is the binding energy, ΔE (kJ mol^{-1}) is the energy relative to the global minimum, N_i is the Hessian index (the number of imaginary intermolecular frequencies), and the geometrical parameters (distances in Å and angles in deg) are given according to the definitions of Figure 1. [b] Ref 30.

TABLE 6: Binding Energy and Geometry of Stationary Point (3) of the Water Dimer Potential Energy Surface Obtained from ab Initio Calculations and Various Polarizable Potentials

structure **3**	E^a	ΔE	N_i	O···O	O···H	α	β
ab initio[b]		2.845	2	2.926	1.971	169.1	115.2
ASP-W	−15.262	4.366	2	3.083	2.127	182.5	120.4
ASP-W2 a	−16.027	5.045	2	3.074	2.118	177.6	119.7
ASP-W2 b	−15.750	5.322	2	2.856	2.171	127.4	88.2
ASP-W2 c	−15.704	5.368	3	2.969	2.131	145.3	100.8
ASP-W4 a	−16.235	4.640	2	3.077	2.120	179.4	121.2
ASP-W4 b	−15.881	4.994	3	2.975	2.132	146.1	104.2
NEMO1	−18.456	2.327	1	2.939	1.985	174.4	113.6
NEMO2	−17.932	1.790	1	2.931	1.976	175.1	115.3
NEMO3	−18.427	1.691	1	2.951	2.002	171.4	108.6
NCC	−20.658	0.673	1	2.970	2.014	176.5	116.8
CKL	−21.269	1.930	1	2.987	2.031	176.0	113.6
SK	−17.987	1.028	1	2.840	1.883	179.2	111.0
POL1	−23.304	0.222	1	2.755	1.755	180.5	107.5
POL2	−22.665	0.221	1	2.787	1.787	180.9	107.8
KJ	−19.684	1.860	1	2.956	2.006	171.5	111.7
PSPC	−17.817	0.193	1	2.856	1.856	181.7	108.3
RER(pol)	−14.450	0.194	1	2.947	1.989	184.8	110.3

[a] See note to Table 5. [b] Ref 30.

In Figure 2, we have reported the stationary points in increasing order of energy for each potential. This figure shows the great diversity of the PES obtained from polarizable potentials. Although some features linked to the molecular shape and the nature of the dominant interactions are shared by all the potentials, details of the topology of the PES are very model-dependent. As the PES of the water dimer is very flat, it is quite difficult to model it accurately. In principle, the introduction of the polarizability must give a more realistic model, but the differences observed between various polarizable water models show that it does not necessarily lead to an improvement in accuracy.

TABLE 7: Binding Energy and Geometry of the Stationary Points (2, 4) of the Water Dimer Potential Energy Surface Obtained from ab Initio Calculations and Various Polarizable Potentials

structure **2**	E^a	ΔE	N_i	O···O	O···H	α_1 $\psi_1{}^c$	α_2 $\psi_2{}^c$	α_3 $\psi_3{}^c$
ab initio[b]		2.803	1	2.926	1.969	113.7	134.7	169.3
						−173.4	−26.5	28.1
ASP-W	−15.702	3.926	2	2.912	2.158	88.1	166.4	134.8
						163.0	−107.9	99.0
ASP-W2	−16.411	4.661	2	2.926	2.132	92.8	162.0	139.4
						169.4	−62.6	84.9
ASP-W4	−16.265	4.610	2	2.897	2.152	90.4	164.5	133.8
						−178.2	76.9	−67.7

structure **4**	E^a	ΔE	N_i	O···O	O···H	α	β	ψ^c
ab initio[b]		5.146	1	2.776	2.266	112.0	68.0	141.3
ASP-W	−17.330	2.298	2	2.895	2.372	113.9	66.1	115.0
ASP-W2	−18.664	2.408	1	2.809	2.336	109.8	70.2	134.0
ASP-W4	−17.571	3.304	1	2.839	2.355	110.8	69.2	136.7
NEMO1	−17.460	3.323	1	2.806	2.225	118.1	61.9	112.8
NEMO2	−15.265	4.457	1	2.869	2.320	115.7	64.3	117.4
NEMO3	−16.721	3.397	1	2.851	2.277	117.7	62.3	127.8
NCC	−17.552	3.779	1	2.858	2.324	114.6	65.4	134.0
CKL	−17.699	5.500	1	2.972	2.311	125.7	54.3	105.5
SK	−13.584	5.431	1	2.864	2.244	121.6	58.4	127.3
KJ	−16.053	5.491	1	3.074	2.472	120.8	59.2	125.6

[a] See note to Table 5. [b] Ref 30. [c] Dihedral angles: ψ_1 = H1b−O1−O2−H2a. ψ_2 = H1a−O1−O2−H2a. ψ_3 = H2b−O2−O1−H2a. ψ = H2b−O2−H2a−O1.

C. Particular Stationary Points. In the following, we discuss the results obtained for some particular stationary points on the PES that have been extensively studied by theoretical calculations.

*1. Minimum Energy ('Linear') Dimer (Structure **1**).* The binding energy of the global minimum (C_s symmetry) is −20.88 kJ mol^{-1} for ASP-W4 and −21.07 for ASP-W2. For the other potentials, the features of the global minimum of the PES were discussed in the original papers and are collected in Table 5 for completeness. All of the potentials (except ASP-W) give the global minimum as the linear C_s dimer (structure **1**), in agreement with the experimental observation. The binding energy ranges from −14.6 for RER(pol) to −23.1 kJ mol^{-1} for CKL. The artifact in ASP-W, leading to a global minimum slightly distorted from the C_s structure and 0.01 kJ mol^{-1} lower in energy, has disappeared in the revised versions ASP-W2 and ASP-W4. There have been numerous ab initio calculations on the linear water dimer, and recent values of the binding energy (kJ mol^{-1}) are −19.7 ± 0.8,[59] −19.8 ± 0.4,[60] −21.3,[61] −18.66,[62] −19.6,[63] −19.9,[64] −19.5,[65] and −20.9 ± 0.4.[66] This last value is probably the most accurate one to date.

*2. Linear Dimer with High Dipole Moment (Structure **1′**).* By rotating the H-donor in structure **1** by 180° around the H-bond, one obtains the structure **1′** , characterized by a larger dipole moment than that of structure **1**. The ASP potentials are the only ones for which this structure is a saddle point. For the other potentials, it is not a stationary point at all. It is interesting to note that this structure has been found in a recent DFT study of the water dimer to be 2.6 kJ mol^{-1} higher in energy than structure **1**[67] (to be compared with the 3.0 kJ mol^{-1} of ASP-W4), but its Hessian index was not reported. The relevance of this particular structure in liquid water has been discussed in detail in an extensive theoretical study of structures

TABLE 8: Binding Energy and Geometry of Stationary Points (4′, 5) of the Water Dimer Potential Energy Surface Obtained from ab Initio Calculations and Various Polarizable Potentials

structure **4′**	E^a	ΔE	N_i	O···O	O···H O···H	α_1 α_2	β_1 β_2	$\psi_1{}^c$ $\psi_2{}^c$	$\psi_3{}^c$
ASP-W	−17.841	1.787	1	2.841	2.343	111.8	66.6	−140.5	
					2.341	111.9	66.4	81.8	−152.7
ASP-W4 a	−17.338	3.537	1	2.864	2.349	109.4	68.5	−89.6	
					2.399	113.1	65.8	151.7	153.7
ASP-W4 b	−17.324	3.551	2	2.873	2.353	110.2	68.6	−101.0	
					2.399	113.6	66.1	148.4	161.4

structure **5**	E^a	ΔE	N_i	O···O	O···H	α	β	$\psi_1{}^c$	$\psi_2{}^c$
ab initio[b]		6.318	2	2.753	2.274	109.6	70.3	162.2	172.2
ASP-W	−16.342	3.286	1	2.839	2.354	110.9	68.9	135.9	171.1
ASP-W2	−17.818	3.254	1	2.789	2.325	109.1	70.7	−141.8	−170.0
ASP-W4	−17.131	3.744	1	2.801	2.339	109.0	70.7	−147.0	−168.3
NEMO1	−15.734	5.049	1	2.841	2.275	117.1	62.9	129.3	175.5
NEMO2	−13.953	5.769	1	2.900	2.365	114.8	65.1	135.7	176.0
NEMO3	−16.008	4.110	2	2.865	2.298	117.1	62.8	152.8	177.3
CKL	−16.124	7.075	1	3.004	2.361	124.1	55.9	122.8	175.4
SK	−13.047	5.968	2	2.883	2.266	121.4	58.5	160.6	−175.4
KJ	−15.319	6.225	1	3.048	2.463	119.3	60.7	147.3	176.7

[a] See note to Table 5. [b] Ref 30. [c] Dihedral angles: ψ_1 = H1b−O1−H1a−O2. ψ_2 = H2b−O2−H2a−O1. ψ_3 = H2a−O2−O1−H1a. ψ_1 = H2b−O2−H2a−O1. ψ_2 = H2a−O2−O1−H1a.

TABLE 9: Binding Energy and Geometry of Stationary Point (5′) of the Water Dimer Potential Energy Surface Obtained from Various Polarizable Potentials

structure **5′**	E^a	ΔE	N_i	O···O	O···H H···O	α_1 α_2	β_1 β_2	$\psi_1{}^b$ $\psi_2{}^b$	$\psi_3{}^b$
ASP-W a	−16.072	3.556	2	2.880	2.374	112.6	67.3	142.0	
					2.374	112.5	67.4	101.6	−172.6
ASP-W b	−16.105	3.523	1	2.872	2.334	114.9	65.2	142.3	
					2.407	109.5	69.2	88.5	−163.8
NEMO1	−15.643	5.140	2	2.855	2.213	123.5	58.6	158.7	
					2.392	109.3	68.4	119.3	−175.0
NEMO2	−13.953	5.769	2	2.900	2.381	113.7	66.0	130.9	
					2.351	115.9	64.4	141.7	−175.9
CKL	−16.045	7.154	2	3.013	2.336	127.2	59.0	155.7	
					2.422	119.6	54.1	112.6	−175.0
KJ	−15.319	6.225	2	3.048	2.468	118.8	61.0	145.2	
					2.457	119.8	60.4	149.8	176.7

[a] See note to Table 5. [b] Dihedral angles: ψ_1 = H1b−O1−H1a−O2. ψ_2 = H2b−O2−H2a−O1. ψ_3 = H2a−O2−O1−H1a.

TABLE 10: Binding Energy and Geometry of Stationary Point (6) of the Water Dimer Potential Energy Surface Obtained from ab Initio Calculations and Various Polarizable Potentials

structure **6**	E^a	ΔE	N_i	O···O	O···H	α
ab initio[b]		6.401	3	2.740	2.276	108.5
ASP-W	−14.199	5.429	3	2.824	2.394	106.8
ASP-W2	−15.689	5.383	3	2.794	2.362	106.9
ASP-W4	−15.869	5.006	3	2.786	2.368	105.9
NEMO1	−15.057	5.726	3	2.870	2.326	115.5
NEMO2	−13.598	6.124	3	2.918	2.398	113.7
NEMO3	−15.957	4.161	3	2.868	2.304	116.9
NCC	−17.182	4.149	2	2.850	2.326	113.8
CKL	−15.439	7.760	3	3.036	2.419	122.0
SK	−13.034	5.981	3	2.885	2.269	121.4
POL1	−17.082	6.444	1	2.822	2.144	123.5
POL2	−16.403	6.483	1	2.860	2.183	123.6
KJ	−15.171	6.373	3	3.026	2.454	118.2
PSPC	−12.590	5.420	1	2.939	2.269	123.3
RER(pol)	−9.950	4.694	1	3.037	2.404	123.1

[a] See note to Table 5. [b] Ref 30.

TABLE 11: Binding Energy and Geometry of Stationary Point (9) of the Water Dimer Potential Energy Surface Obtained from ab Initio Calculations and Various Polarizable Potentials

structure **9**	E^a	ΔE	N_i	O···O	O···H	α
ab initio[b]		7.238	1	2.944	2.452	111.4
ASP-W	−13.836	5.792	1	2.987	2.518	110.2
ASP-W2	−14.712	6.360	1	2.979	2.510	110.2
ASP-W4	−15.142	5.733	1	2.970	2.502	110.1
NEMO1	−12.304	8.479	1	3.035	2.564	110.6
NEMO2	−12.054	7.668	1	3.058	2.585	110.7
NEMO3	−11.179	8.939	1	3.075	2.602	110.8
NCC	−14.867	6.464	1	3.017	2.546	110.4
CKL	−10.625	12.574	1	3.225	2.745	111.7
SK	−11.110	7.905	1	3.029	2.558	110.5
POL1	−13.762	9.764	1	2.987	2.544	106.5
POL2	−13.547	9.339	1	3.019	2.574	106.8
KJ	−11.030	10.514	1	3.238	2.758	111.8
PSPC	−11.088	6.922	1	3.073	2.625	107.1
RER(pol)	−10.859	3.785	1	3.109	2.633	111.0

[a] See note to Table 5. [b] Ref 30.

1 and **1′** of the water dimer in a cavity model,[68] where structure **1′** has been found to be a local minimum.

*3. Planar Cyclic Dimer (Structure **6**).* This stationary point has been studied many times by theoretical calculations, as have the linear and bifurcated ones.[69,70] SSPSR[30] found it to be an index-3 stationary point, lying 6.4 kJ mol^{-1} above the global minimum and 0.8 kJ mol^{-1} below the bifurcated dimer. ASP-W, ASP-W2, NEMO2, CKL, and KJ are in good agreement with the ab initio result. NCC finds it to have index 2 and to be only 4.1 kJ mol^{-1} above the global minimum. With POL2, PSPC, and RER(pol), the planar cyclic dimer is a true saddle point.

*4. Bifurcated Dimer (Structure **9**).* The geometry obtained by the ASP, NEMO, NCC, and POL2 potentials appears to be satisfactory. The energy relative to the global minimum is in good agreement with the ab initio result for all the potentials,

TABLE 12: Binding Energy and Geometry of Stationary Point (7) of the Water Dimer Potential Energy Surface Obtained from ab Initio Calculations and Various Polarizable Potentials

structure **7**	E^a	ΔE	N_i	O···O	O···H	O···H	α	β
ab initio[b]		9.247	2	2.871	2.620	2.570	95.1	61.3
ASP-W	−13.599	6.029	2	2.956	3.172	2.523	68.3	35.8
ASP-W2	−14.005	7.067	2	2.947	3.069	2.542	73.7	42.8
ASP-W4	−14.274	6.601	2	2.934	3.004	2.537	76.6	44.7
NEMO1	−11.471	9.312	2	2.998	2.940	2.601	84.1	45.2
NEMO2	−10.927	8.795	2	3.029	2.891	2.661	89.0	50.4
NEMO3	−10.779	9.339	2	3.045	3.058	2.630	80.2	41.6
NCC	−13.242	8.089	2	2.986	2.774	2.637	93.3	53.2
CKL	−10.297	12.902	2	3.207	3.245	2.766	79.2	36.1
SK	−9.701	9.314	2	3.010	2.752	2.650	96.2	51.6
POL1	−11.520	12.006	2	2.976	2.953	2.567	102.6	60.0
POL2	−11.195	11.691	2	3.012	2.612	2.736	103.8	60.8
KJ	−10.575	10.969	2	3.251	3.232	2.827	82.7	40.4
PSPC	−8.897	9.113	2	3.074	2.643	2.812	106.1	62.5
RER(pol)	−7.851	6.793	2	3.140	2.637	2.920	113.1	68.6

[a] See note to Table 5. [b] Ref 30.

TABLE 13: Binding Energy and Geometry of the Stationary Points (10, 10′) of the Water Dimer Potential Energy Surface Obtained from ab Initio Calculations and Various Polarizable Potentials

structure **10**	E^a	ΔE	N_i	O···O	O···H	α
ab initio[b]		12.803	2	3.126	2.630	112.3
ASP-W	−9.948	9.680	3	3.131	2.655	111.2
ASP-W2	−10.921	10.151	3	3.107	2.632	111.0
ASP-W4	−10.918	9.957	3	3.115	2.640	111.1
NEMO1	−9.420	11.363	2	3.162	2.685	111.4
NEMO2	−9.293	10.429	2	3.189	2.710	111.5
NEMO3	−8.776	11.342	2	3.196	2.717	111.6
NCC	−12.265	9.066	2	3.099	2.625	111.0
CKL	−8.530	14.669	2	3.292	2.810	112.1
SK	−9.529	9.486	2	3.088	2.614	110.9
POL1	−12.317	11.209	2	3.026	2.581	106.8
POL2	−12.165	10.721	2	3.057	2.610	107.0
KJ	−8.828	12.716	2	3.315	2.832	112.2
PSPC	−10.015	7.995	2	3.109	2.660	107.4
RER(pol)	−10.099	4.545	2	3.138	2.661	111.2

structure **10′**	E^a	ΔE	N_i	O···O	O···H	α_1	α_2
ASP-W	−10.412	9.216	2	3.089	2.622	52.2	172.2
ASP-W2	−11.309	9.763	2	3.076	2.608	47.1	173.0
ASP-W4	−11.021	9.854	2	3.101	2.629	35.9	175.1

[a] See note to Table 5. [b] Ref 30.

except for RER(pol) (too low) and CKL and KJ (too high). All the potentials used find the bifurcated dimer to be a true saddle point (index 1). One published ab initio calculation has found structure **9** to be a minimum,[71] but it seems now that it is definitely a saddle point.[72]

An MP2 study by Vos et al. with two basis sets (DZP′ and ESPB) finds the cyclic and bifurcated dimers respectively about 3.7−4.3 and 6.9−8.0 kJ mol^{-1} above the global minimum.[70] This is in acceptable agreement with SSPSR, who found energy differences of 6.4 and 7.2 kJ mol^{-1}, respectively. The results for the intermolecular potentials are more scattered, but the energy order is consistent, except for the RER(pol) potential, which finds the bifurcated structure to be lower than the planar cyclic one by 0.9 kJ mol^{-1}.

*5. Triply-Hydrogen-Bonded Dimer (Structure **7**).* SSPSR[30] found this structure to be an index-2 stationary point lying 9.2 kJ mol^{-1} above the global minimum. All the polarizable potentials considered find a corresponding index-2 structure, and ASP and RER(pol) find it to be significantly nearer in energy to the global minimum, while CKL, POL1, and POL2 place it significantly higher.

TABLE 14: Binding Energy and Geometry of the Stationary Points (8, 9′) of the Water Dimer Potential Energy Surface Obtained from ab Initio Calculations and Various Polarizable Potentials

structure **8**	E^a	ΔE	N_i	O···O	O···H	α
ab initio[b]		18.577	3	3.385	3.144	60.1
ASP-W	−8.530	11.098	3	3.086	2.911	67.1
ASP-W2	−8.684	12.388	3	3.096	2.954	71.1
ASP-W4	−8.226	12.649	3	3.118	2.973	70.7
NEMO1	−4.551	16.232	3	3.379	3.230	70.8
NEMO2	−4.554	15.168	3	3.442	3.280	71.5
NEMO3	−4.746	15.372	3	3.355	3.219	72.2
NCC	−6.064	15.267	3	3.268	3.129	71.7
CKL	−4.821	18.378	3	3.411	3.235	67.6
SK	−5.115	13.900	3	3.216	3.081	72.1
POL1	−6.616	16.910	3	3.145	2.963	76.9
POL2	−6.500	16.386	3	3.180	3.108	76.9
KJ	−5.373	16.171	3	3.549	3.370	67.5
PSPC	−5.252	12.758	3	3.242	3.171	77.2
RER(pol) a	−5.255	9.389	3	3.332	3.249	77.9
RER(pol) b	−4.933	9.711	3	4.093	4.019	79.7

structure **9′**	E^a	ΔE	N_i	O···O	O···H	α
CKL	−1.562	21.637	2	3.127	2.652	111.2

[a] See note to Table 5. [b] Ref 30.

*6. Doubly-Bifurcated Dimer (Structure **8**).* From the ab initio calculation, this structure with four H-bonds is an index-3 stationary point lying 18.6 kJ mol^{-1} higher than the global minimum. As for the triply-hydrogen-bonded dimer, all the potentials considered agree with this characterization. With the ASP potentials, this stationary point is lower in energy, by about 6.5 kJ mol^{-1}, and the intermolecular distances are shorter. PSPC and RER(pol) also find a lower energy for this structure. For RER(pol) we found two structures of this type **8** (reported in Table 1) plus a third one, lying 0.003 kJ mol^{-1} higher than the one at −4.933 kJ mol^{-1}, with a very similar geometry but a Hessian index of 4. This particular structure is most probably an artifact of the numerical calculations and has not been reported in Table 14.

D. Intermolecular Vibrational Frequencies. As the water molecules are treated as rigid bodies, each molecule in the dimer has six degrees of freedom: three translations and three rotations. The intermolecular normal modes and their frequencies were obtained by diagonalization of the 12 × 12 *GF* matrix.[56,73]

Table 15 gives the harmonic frequencies for each of the intermolecular modes of the minimum energy dimer for the polarizable potentials studied, together with some ab initio results.[74−76] Experimental frequencies are also given, although they are not directly comparable because they are fundamental frequencies and because they were measured for the dimer in a nitrogen matrix.[77] The frequencies are grouped by symmetry and given in order of decreasing frequency for each symmetry. Of the three *A*′ modes, the highest-frequency one is normally the in-plane H-bond shear (in the terminology of Owicki et al.[78]), which is an "antigeared" bending motion, the next is the in-plane H-bond bend, which is a "geared" bending motion, and the lowest-frequency mode is the H-bond stretch. Of the *A*″ modes, the highest-frequency mode is an out-of-plane shear ("antigeared"), the next is an H-bond torsion, and the lowest-frequency mode is an out-of-plane bend ("geared"). These are illustrated in ref 78, and animated illustrations of the modes for ASP-W4 can be viewed by users of the World Wide Web.[79]

Most potentials and ab initio calculations overestimate the *A*′ and *A*″ shear mode frequencies and underestimate the *A*′

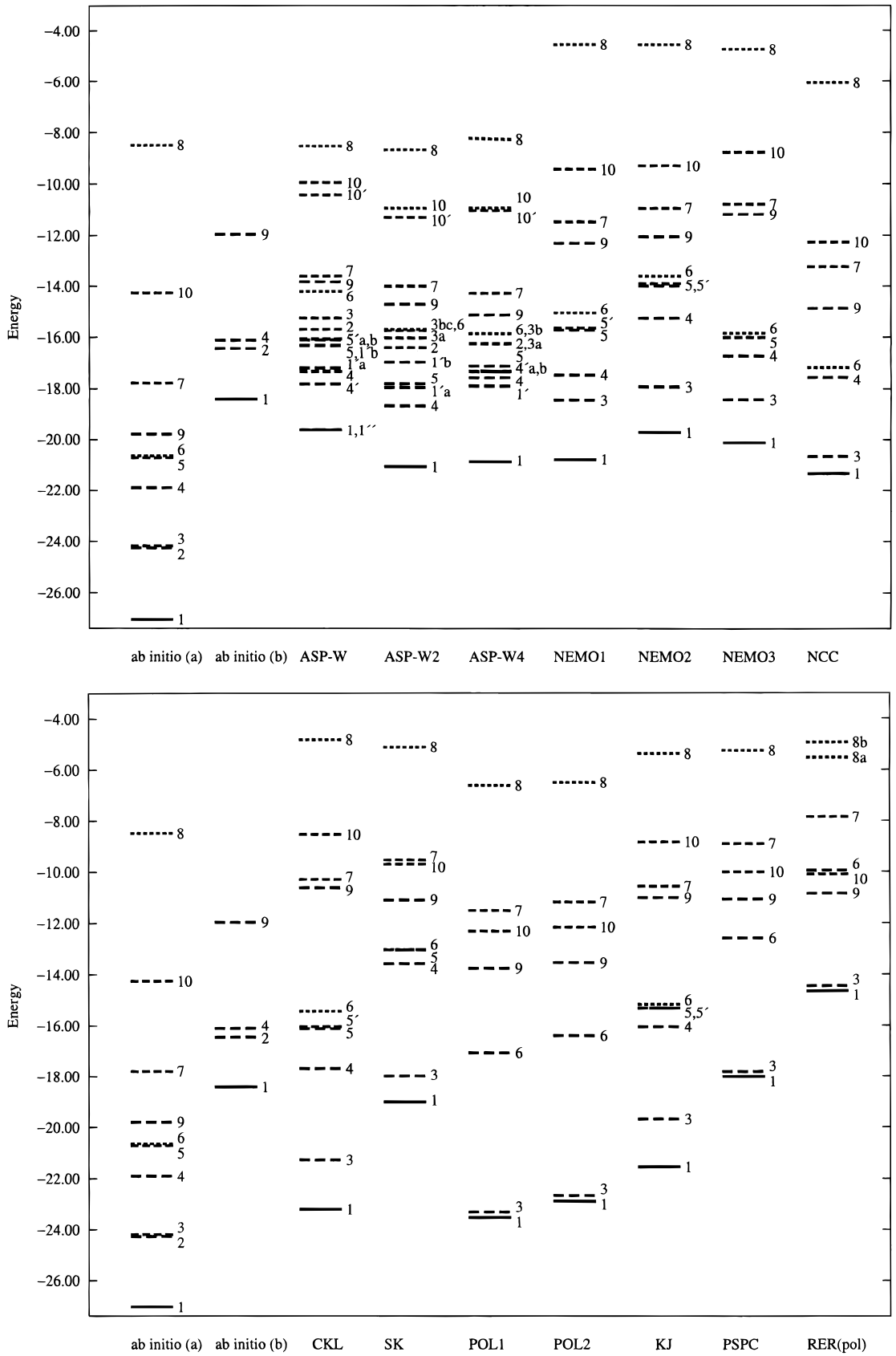

Figure 2. Hierarchy of the stationary points of the water dimer potential energy surface for various intermolecular potentials including polarizability, and ab initio results of SSPSR:[30] (a) MP2/6-31G+G(d,p) level, (b) idem., including an estimated BSSE correction. The numbers refer to structures of Figure 1. For each structure, the line style symbolizes the Hessian index: (—) $N_i = 0$; (− − −) $N_i = 1$; (- - -) $N_i = 2$; (···) $N_i = 3$.

stretch frequency. The same assignment is generally found, except for the empirical potentials KJ, POL1, POL2, PSPC, and RER(pol), for which the A'' torsion has lower frequency than the A' bend. The best values for the shear modes are those obtained by the NCC potential. ASP-W4 gives the best agreement with the experimental value for the A' bend frequency.

TABLE 15: Intermolecular Fundamental Frequencies (cm^{-1}) of the Water Dimer $(H_2O)_2$ in an N_2 Matrix, and Harmonic Frequencies Calculated ab Initio and Using Polarizable Intermolecular Potentials. The Modes are Grouped According to Symmetry and Listed in Order of Decreasing Frequency

	A′			*A″*		
experiment[a]	320	243	155	520		
DFT-BP[b]	393	205	145	663	159	137
HF/6-31G**[c]	375	175	142	605	145	121
HF/6-31G ext.[c]	356	174	142	589	153	129
HF[d]	362	187	146	649	166	145
MP2[d]	398	220	178	715	193	155
ASP-W	393	187	151	555	181	54
ASP-W2	426	189	130	543	139	41
ASP-W4	408	192	177	566	147	83
NCC	299	166	114	510	125	90
NEMO1	403	214	127	627	168	117
NEMO2	371	189	128	599	168	116
NEMO3	406	205	135	609	141	109
CKL	445	254	142	678	189	107
SK	358	198	129	556	136	92
POL1	410	218	182	633	148	46
POL2	402	213	181	623	148	46
KJ	384	204	170	592	169	107
PSPC	345	186	162	539	132	45
RER(pol)	292	160	148	471	126	43

[a] Experimental results, ref 77. [b] DFT calculation, harmonic frequencies, ref 74. [c] Hartree−Fock calculation, harmonic frequencies, ref 75. [d] 6-31G* basis plus diffuse function on oxygen, harmonic frequencies, ref 76.

IV. Interchange of Hydrogen Atoms in the Water Dimer

A. General Considerations. The molecular symmetry group of the water dimer comprises 16 operations, generated as follows. For molecule *A*, the O atom is labeled *a* and the H atoms 1 and 2. Similarly the atoms of molecule *B* are *b*, 3, and 4. Then the symmetry group is generated by the permutation (*ab*)(13)(24) that exchanges the two molecules, the permutations (12) and (34) that exchange the H atoms within each molecule, and the inversion E^* of the entire system in the center of mass. The equilibrium geometry has C_s symmetry, containing only two operations, so there are $8 = 16/2$ equivalent versions of the global minimum structure **1** of the water dimer.[80] All of these versions are connected by low-energy paths on the PES, one corresponding to interchange of hydrogens in the proton acceptor and the other to interchange of donor and acceptor.[81] These paths pass through the saddle points (index-1 stationary points) of the PES, which therefore play a central role in understanding the rotational and vibrational spectra of the water dimer.[30,33,82]

B. Interchange of Hydrogen Atoms in the Acceptor Molecule. This interchange corresponds to an internal motion around an unbroken H-bond. Smith et al. find a pathway through structure **2** ($N_i = 1$) with a barrier height equal to 2.80 kJ mol^{-1} at the MP2/6-31+G(d,p) level, their best estimate being 2.47 kJ mol^{-1}. Wales found a barrier of 2.1 kJ mol^{-1} through structure **2** at the BSSE-corrected MP2/DZP+diff level.[33]

For the polarizable potentials we have considered, structure **2** is found to be a stationary point ($N_i = 2$) only for the ASP potentials. According to ASP-W4 there are two stationary points with structure **3**; one of these corresponds to the ab initio structure **3** and, like it, has $N_i = 2$; the other has a more strongly bent hydrogen bond and $N_i = 3$. ASP-W2 finds the same two structures, with slightly different geometrical parameters, and a third that has a very strongly bent hydrogen bond and $N_i = 2$. For all the other potentials, structure **3** is a saddle point, and no stationary point has been found corresponding to structure **2**. The barrier **1** → **3** is found to be close to 0.2 kJ mol^{-1} for POL1, POL2, PSPC, and RER(pol), 0.67 kJ mol^{-1} for NCC, and 1.03 kJ mol^{-1} for SK, values that seem to be much too small. For the ASP potentials, transitions through structures **2** or **3** occur with higher energy barriers (4−5 kJ mol^{-1}).

C. Interchange of Donor and Acceptor Molecules. According to Smith et al., the minimum energy pathway is through structure **4** with a barrier of 3.64 kJ mol^{-1} for their best estimate. Wales reports a barrier of 2.4 kJ mol^{-1} through the same transition state.[33]

For the intermolecular potentials POL1, POL2, PSPC, and RER(pol), there are no stationary points with this structure. For the ASP potentials, structure **4** and related structures **4′**, **5**, and **5′** have lower energy than structures **2** or **3**, which is a point of disagreement with the ab initio results of Smith et al. The other potentials give results more in line with the ab initio study, uncorrected for BSSE, where structure **4** is higher in energy than structure **3** by about 2 kJ mol^{-1}. However, SSPSR have estimated the BSSE correction for structures **3** and **4**, and this correction brings these structures very close in energy (0.5 kJ mol^{-1}).

We note that although structures **5** and **5′** are stationary points for ASP-W, NEMO1, NEMO2, CKL, and KJ, no stationary point with structure **5** is found for SK, NEMO3, and ASP-W2, and neither of these stationary points is found for NCC, POL1, POL2, PSPC, and RER(pol).

Structure **6** is also close in energy to structures of types **4**, **4′**, **5**, and **5′** and has index 3 for all the potentials except POL1, POL2, PSPC, and RER(pol), for which $N_i = 1$, and surprisingly NCC for which $N_i = 2$.

The barrier height through structure **4** varies from 2.3 to 5.5 kJ mol^{-1} depending on the potential.

D. Interchange of Hydrogen Atoms in the Donor Molecule. This pathway has a barrier through structure **9** equal to 7.87 kJ mol^{-1} according to SSPSR (best estimate) and 5.7 kJ mol^{-1} according to Wales (BSSE-corrected MP2/DZP+diff level). ASP-W4 agrees well with the latter value.

For the polarizable potentials, structure **9** is a true saddle point, but its energy varies between 3.8 and 12.6 kJ mol^{-1} above the minimum energy dimer.

V. Second Virial Coefficient

A. Theory. The Helmholtz free energy of a real gas composed of asymmetric top molecules at sufficiently low density can be written[83−85]

$$F = F_{\mathrm{id}} - kT\frac{N^2}{2V}\int \langle e^{-U_{12}/kT} - 1\rangle_{\omega_1\omega_2}\,\mathbf{dr} + \frac{N\hbar^2}{24(kT)^2}\left[\frac{\langle \mathbf{F}^2\rangle}{M} + \sum_{\alpha}\frac{\langle T_\alpha{}^2\rangle}{I_{\alpha\alpha}}\right] - \frac{N\hbar^2}{24}\sum_{\mathrm{cyclic}}\left(\frac{2}{I_A} - \frac{I_A}{I_B I_C}\right) + O(\hbar^4) \quad (6)$$

where U_{12} is the potential energy of a pair, **F** the force on one molecule, *M* the molecular mass, and T_α the component in the molecular inertial axis reference frame of the torque about the α axis of one molecule for which the moment of inertia is $I_{\alpha\alpha}$. The first term on the right-hand side of eq 6 is the ideal gas

TABLE 16: Experimental Values (cm³ mol⁻¹) of the Second Virial Coefficient $B(T)$ of Water vs T (K) from Various Sources. The Numbers in Parentheses Give Estimates of the Error

	year					
T (K)	1967−68 *a*	1984 *b*	1988 *c*	1988 *d*	1989 *e*	1995 *f*
273.2		−1782.8	−1855.6			−1723.3
323.2		−801.7	−816.1			−815.4
373.2	−580	−452.7	−454.0	−451.0(18)		−458.6
423.2	−330(5)	−292.0	−291.8	−288.1(10)	−275.0(7)	−293.8
448.2	−264(2)			−240.6(4)	−239.5(6)	−243.9
473.2	−211(4)	−204.1	−205.4	−203.0(2)	−200.8(1)	−206.2
523.2			−151.9		−149.8(0.3)	−153.4
573.2	−117.5(0.5)	−115.1	−117.1		−115.8(0.5)	−118.5
623.2		−90.6				−93.6
673.2	−73.4(0.1)				−73.5(0.3)	−75.1
723.2		−59.1				−60.7
773.2					−49.9(0.3)	−49.4
873.2						−33.1
973.2						−22.5

a Ref 40, 41. *b* Ref 42, quoted by Guissani and Guillot.[34] *c* Ref 92. *d* Ref 87. *e* Ref 43. *f* Ref 93.

contribution, the second is the classical term due to the intermolecular interactions assumed to be limited to interactions of pairs, an approximation valid at low density, and the last two terms are the quantum corrections to order $\hbar^2$.

The pressure is defined by

$$P = -\left(\frac{\partial F}{\partial V}\right)_{N,T} \tag{7}$$

and the virial expansion

$$P = \frac{NkT}{V}\left[1 + \frac{N}{V}B(T) + \left(\frac{N}{V}\right)^2 C(T) + ...\right] \tag{8}$$

leads to the definition of the virial coefficients.

At low density, the virial expansion can be truncated at the second term, and we have

$$F = F_{id} + \frac{N^2kT}{V}B(T) \tag{9}$$

with

$$B(T) = -\frac{1}{2}\int \langle e^{-U_{12}/kT} - 1\rangle_{\omega_1\omega_2}\, d\mathbf{r} + \frac{\hbar^2}{24(kT)^3}\left[\frac{\langle \mathbf{F}^2\rangle_0}{M} + \sum_\alpha \frac{\langle T_\alpha{}^2\rangle_0}{I_{\alpha\alpha}}\right] \tag{10}$$

where $\langle\ \rangle_0$ means the low density limit of $\langle\ \rangle/\rho$, with ρ the number density.

$B(T)$ can thus be written as the sum of the classical second virial coefficient

$$B_{cl}(T) = -\frac{1}{2}\int \langle e^{-U_{12}/kT} - 1\rangle_{\omega_1\omega_2}\, d\mathbf{r} \tag{11}$$

and the translational and rotational first quantum corrections

$$\Delta B_{qu}^{trans}(T) = \frac{\hbar^2}{24(kT)^3}\frac{\langle \mathbf{F}^2\rangle_0}{M}$$

$$\Delta B_{qu}^{rot}(T) = \frac{\hbar^2}{24(kT)^3}\sum_\alpha \frac{\langle T_\alpha{}^2\rangle_0}{I_{\alpha\alpha}} \tag{12}$$

B. Calculation Details. Monte Carlo numerical integration was used to evaluate the multidimensional integrals arising in eqs 11 and 12. The distance R between the molecular centers of mass is varied from 0.075 to 45 au in steps of 0.075 au; for each value, 10 000 orientations of both molecules are chosen at random to evaluate the orientationally averaged Mayer

TABLE 17: Classical Second Virial Coefficient $B_{cl}(T)$ of Water for Various Polarizable Potentials and the Experimental Results. Values Are Given in cm³ mol⁻¹. R_d Is the Minimum Distance between the Centers of Mass Required To Avoid the Multipolar Catastrophe

T/K	ASP−W	ASP−W2	ASP−W4	NEMO1	NEMO2	NEMO3	NCC	expt[a]
373.2	−448.0	−528.4	−505.0	−372.4	−315.9	−351.3	−594.7	
423.2	−288.1	−331.4	−318.8	−231.1	−200.2	−220.3	−358.4	−275.0
448.2	−239.0	−272.4	−262.7	−188.3	−164.3	−180.0	−289.9	−239.5
473.2	−201.6	−228.1	−220.4	−155.9	−136.7	−149.5	−239.3	−200.8
523.2	−149.3	−166.8	−161.6	−110.7	−97.7	−106.5	−170.7	−149.8
573.2	−114.8	−127.2	−123.4	−81.3	−71.9	−78.3	−127.4	−115.8
673.2	−73.2	−80.1	−77.8	−46.2	−40.5	−44.2	−77.2	−73.5
773.2	−49.5	−53.8	−52.3	−26.5	−22.6	−24.9	−50.0	−49.9
873.2	−34.5	−37.4	−36.2	−14.4	−11.4	−12.8	−33.2	
973.2	−24.3	−26.3	−25.4	−6.8	−3.9	−4.6	−22.1	
R_d/Å	1.5	1.5	2.3	2.3	2.4	2.7	2.0	

T/K	CKL	SK	POL1	POL2	KJ	PSPC	RER(pol)	expt[a]
373.2	−536.7	−228.1	−480.6	−434.6	−484.8	−200.2	−261.1	
423.2	−321.0	−147.8	−288.9	−266.5	−308.3	−133.3	−192.5	−275.0
448.2	−259.1	−122.2	−233.7	−217.1	−255.1	−111.5	−168.3	−239.5
473.2	−213.5	−102.4	−192.9	−180.2	−215.0	−94.4	−148.6	−200.8
523.2	−152.0	−74.0	−137.6	−129.5	−159.2	−69.3	−118.5	−149.8
573.2	−113.2	−54.8	−102.4	−97.0	−122.7	−52.1	−96.7	−115.8
673.2	−68.1	−31.0	−61.5	−58.5	−78.7	−30.3	−67.5	−73.5
773.2	−43.5	−17.2	−39.0	−37.0	−53.6	−17.4	−49.1	−49.9
873.2	−28.2	−8.4	−25.0	−23.5	−37.6	−9.0	−36.5	
973.2	−18.0	−2.4	−15.7	−14.5	−26.6	−3.2	−27.5	
R_d/Å	2.5	0.1	2.6	2.6	1.5	1.5	1.4	

a Ref 43.

TABLE 18: Second Virial Coefficient ($cm^3\ mol^{-1}$) $B(T)$ of Water, Including Quantum Corrections, for Various Polarizable Potentials, and the Experimental Results

T/K	ASP-W	ASP-W2	ASP-W4	NEMO1	NEMO2	NEMO3	NCC	expt[a]
373.2	−381.8	−444.3	−415.0	−301.1	−260.5	−287.2	−496.6	
423.2	−255.5	−291.4	−275.7	−196.4	−172.0	−188.4	−312.9	−275.0
448.2	−214.8	−243.2	−231.1	−162.6	−143.0	−156.3	−257.0	−239.5
473.2	−183.2	−206.1	−196.5	−136.3	−120.3	−131.2	−214.7	−200.8
523.2	−137.8	−153.4	−147.0	−98.5	−87.3	−95.0	−155.9	−149.8
573.2	−107.1	−118.3	−113.7	−73.2	−64.8	−70.5	−117.7	−115.8
673.2	−69.2	−75.6	−72.9	−41.9	−36.6	−40.1	−72.4	−73.5
773.2	−47.1	−51.2	−49.3	−24.0	−20.3	−22.4	−47.1	−49.9
873.2	−33.0	−35.7	−34.3	−12.7	−9.8	−11.2	−31.4	
973.2	−23.3	−25.1	−24.0	−5.6	−2.7	−3.5	−20.9	

T/K	CKL	SK	POL1	POL2	KJ	PSPC	RER(pol)	expt[a]
373.2	−421.5	−192.8	−394.6	−362.0	−409.8	−175.7	−246.0	
423.2	−269.7	−129.5	−250.5	−233.3	−272.8	−120.3	−183.7	−275.0
448.2	−222.5	−108.4	−206.3	−193.2	−229.3	−101.5	−161.4	−239.5
473.2	−186.6	−91.7	−172.7	−162.4	−195.5	−86.5	−143.1	−200.8
523.2	−136.1	−67.1	−125.4	−118.9	−147.3	−64.2	−114.7	−149.8
573.2	−103.0	−50.1	−94.7	−90.1	−114.8	−48.5	−94.0	−115.8
673.2	−63.1	−28.5	−57.6	−55.0	−74.7	−28.3	−66.0	−73.5
773.2	−40.6	−15.6	−36.7	−34.9	−51.2	−16.2	−48.1	−49.9
873.2	−26.4	−7.3	−23.6	−22.2	−36.1	−8.2	−35.9	
973.2	−16.7	−1.6	−14.7	−13.5	−25.6	−2.6	−27.0	

[a] Ref 43.

TABLE 19: Details of the Quantum Corrections for the Second Virial Coefficient $B(T)$ ($cm^3\ mol^{-1}$) of Water for Some Polarizable Potentials. $\Delta B_{qu}^{trans}(T)$ and $\Delta B_{qu}^{rot}(T)$ Are the Corrections Arising from Translational and Rotational Molecular Degrees of Freedom, Respectively

T/K	ASP-W	ASP-W2	ASP-W4	NEMO1	NEMO2	NEMO3	NCC	CKL
				$\Delta B_{qu}^{trans}(T)$				
373.2	5.0	6.3	5.9	4.5	3.2	3.8	6.9	10.2
423.2	2.4	3.0	2.8	2.2	1.6	1.9	3.2	4.6
448.2	1.8	2.2	2.1	1.6	1.2	1.4	2.3	3.3
473.2	1.4	1.6	1.6	1.2	0.9	1.1	1.7	2.4
523.2	0.9	1.0	1.0	0.7	0.6	0.7	1.0	1.4
573.2	0.6	0.7	0.7	0.5	0.4	0.5	0.7	0.9
673.2	0.3	0.4	0.3	0.3	0.2	0.3	0.3	0.5
773.2	0.2	0.2	0.2	0.2	0.1	0.2	0.2	0.3
873.2	0.1	0.1	0.1	0.1	0.1	0.1	0.1	0.2
973.2	0.1	0.1	0.1	0.1	0.1	0.1	0.1	0.1
				$\Delta B_{qu}^{rot}(T)$				
373.2	61.2	77.7	84.1	66.8	52.2	60.3	91.2	105.0
423.2	30.1	36.9	40.3	32.5	26.6	30.0	42.3	46.7
448.2	22.3	27.0	29.5	24.1	20.0	22.3	30.7	33.3
473.2	17.0	20.4	22.3	18.4	15.4	17.2	22.9	24.5
523.2	10.6	12.4	13.7	11.5	9.9	10.8	13.8	14.5
573.2	7.1	8.2	9.0	7.6	6.7	7.3	9.0	9.3
673.2	3.7	4.1	4.6	4.0	3.6	3.8	4.5	4.5
773.2	2.2	2.4	2.7	2.3	2.2	2.3	2.6	2.6
873.2	1.4	1.6	1.8	1.6	1.5	1.5	1.7	1.6
973.2	1.0	1.1	1.2	1.1	1.0	1.0	1.2	1.1

function $f(R) = \langle \exp(-U_{12}(R)/kT) - 1 \rangle_{\omega_1\omega_2}$, the mean square force $\langle \mathbf{F}^2 \exp(-U_{12}(R)/kT) \rangle_{\omega_1\omega_2}$, and the mean square torque $\langle T_\alpha^2 \exp(-U_{12}(R)/kT) \rangle_{\omega_1\omega_2}$. The three contributions to the virial coefficient are then obtained by numerical integration of these functions of R.

We have recently repeated some of these calculations using a Sobol' quasi-random sequence[86] of orientations instead of a random sequence. This gives much more uniform coverage of the configuration space and faster convergence, with an error more nearly proportional to N^{-1} for N points than to $N^{-1/2}$. The ASP-W2 and ASP-W4 values have all been recalculated this way, but for potentials where the calculated values are far from experimental we have not thought it necessary.

For polarizable potentials, an additional problem arises in such calculations. At very short range, where the potential should be repulsive, a notorious divergence in the computation of the induced moments can occur. This will inevitably occur with potentials in which the induction interactions are not damped at short range. This is the case for all the potentials used in the present work, except SK and the three ASP potentials. The SK potential takes into account the overlap of the charge distributions at short range and automatically damps the electrostatic and induction interactions. The ASP potentials use an explicit damping function for the induction interactions, which ensures that the induction energy remains finite at all distances, but it still becomes unphysically large and negative at short distances before approaching zero as $R \rightarrow 0$. Evidently the damping is not satisfactory at such small separations, though it appears to be reasonable at thermally accessible distances. Divergences in the energy also arise from the multipole expansion of the electrostatic interaction, which is not damped like the induction and dispersion (though a penetration term is included in the repulsion term), and for the ASP potentials, such divergences become troublesome at intermolecular distances

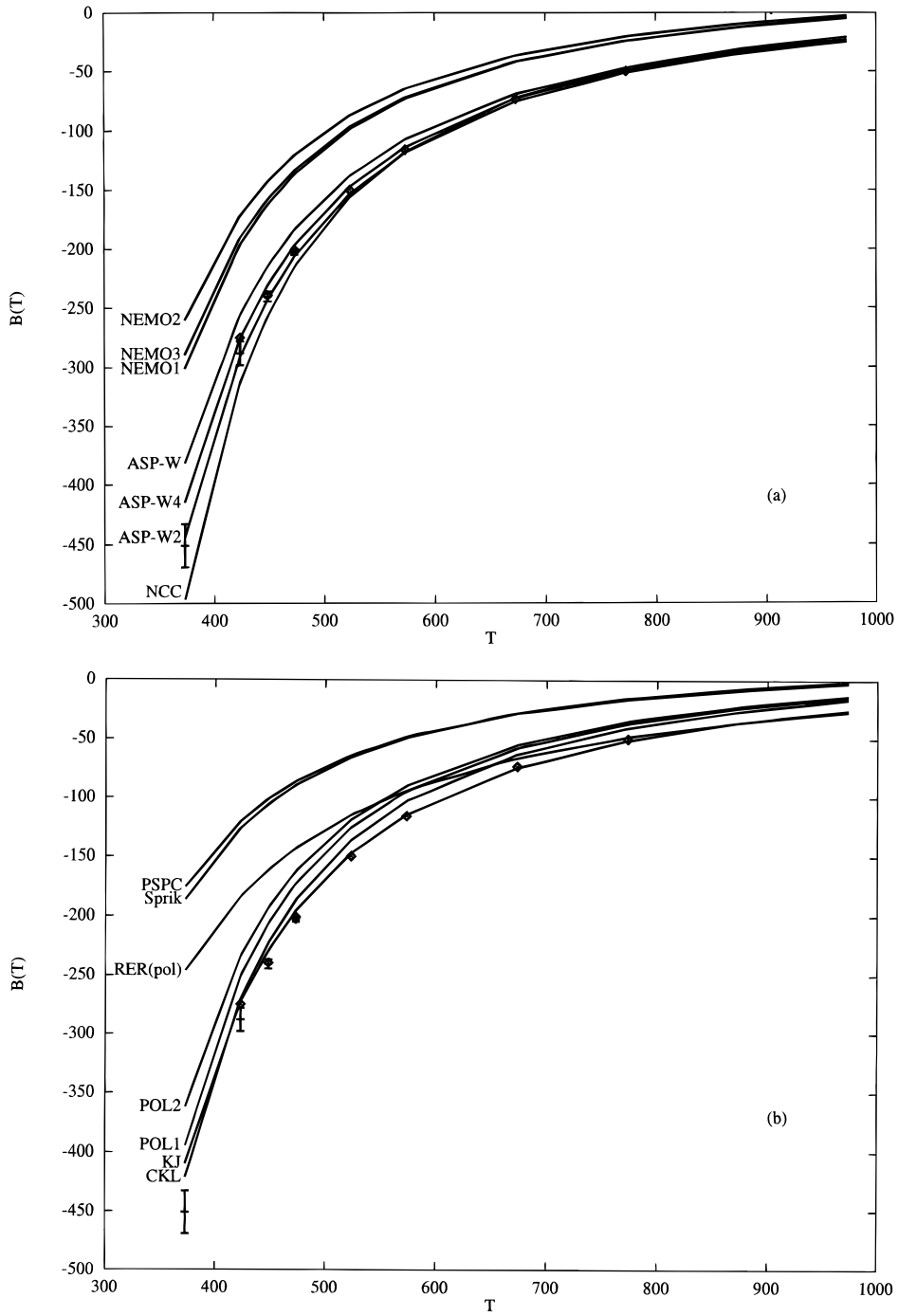

Figure 3. Second virial coefficient $B(T)$ of water including first-order quantum corrections ($cm^3\ mol^{-1}$) for some polarizable intermolecular potentials. The experimental values of ref 87 (set III) are shown by error bars, and those of ref 43 by diamonds. (a) ASP-W, ASP-W2, ASP-W4, NCC, and NEMO1−3; (b) PSPC, POL1−2, RER(pol), SK, CKL, and KJ.

shorter than about 2 Å. For each polarizable model, we indicate in Table 17 the distance R_d between the centers of mass, below which divergence of the potential energy becomes troublesome.

When the potential is sufficiently repulsive, the orientationally averaged Mayer function $f(R)$ is constant and equal to -1. For the polarizable potentials, we have set $f(R) = -1$ for intermolecular distances less than R_d to bypass the divergence problem. This proved to be effective for all the models except POL1, POL2, and NEMO3, for which the potential was not sufficiently repulsive at R_d. For these potentials the problem of the induction divergence can occur at intermolecular distances where the potential is not strongly repulsive. In such cases, we defined the distance R_d' at which $f(R)$ starts to deviate from -1 and $f(R)$ has been linearly interpolated between R_d' and R_d for the integration over R.

C. Results. Experimental results for $B(T)$ from various groups are given in Table 16. There is some doubt about the best values; the last column gives values calculated from the fitted function in the CRC Handbook, for which no source is cited. The scatter between the different sets of values in Table 16 is attributed by Eubank et al.[87] to systematic errors in the experiments caused by adsorption of water on the walls of the apparatus, which leads to values that are too low. Kell et al., in their 1989 experiments,[43] took great care to avoid errors from this source, and their results are likely to be more reliable than the earlier ones.

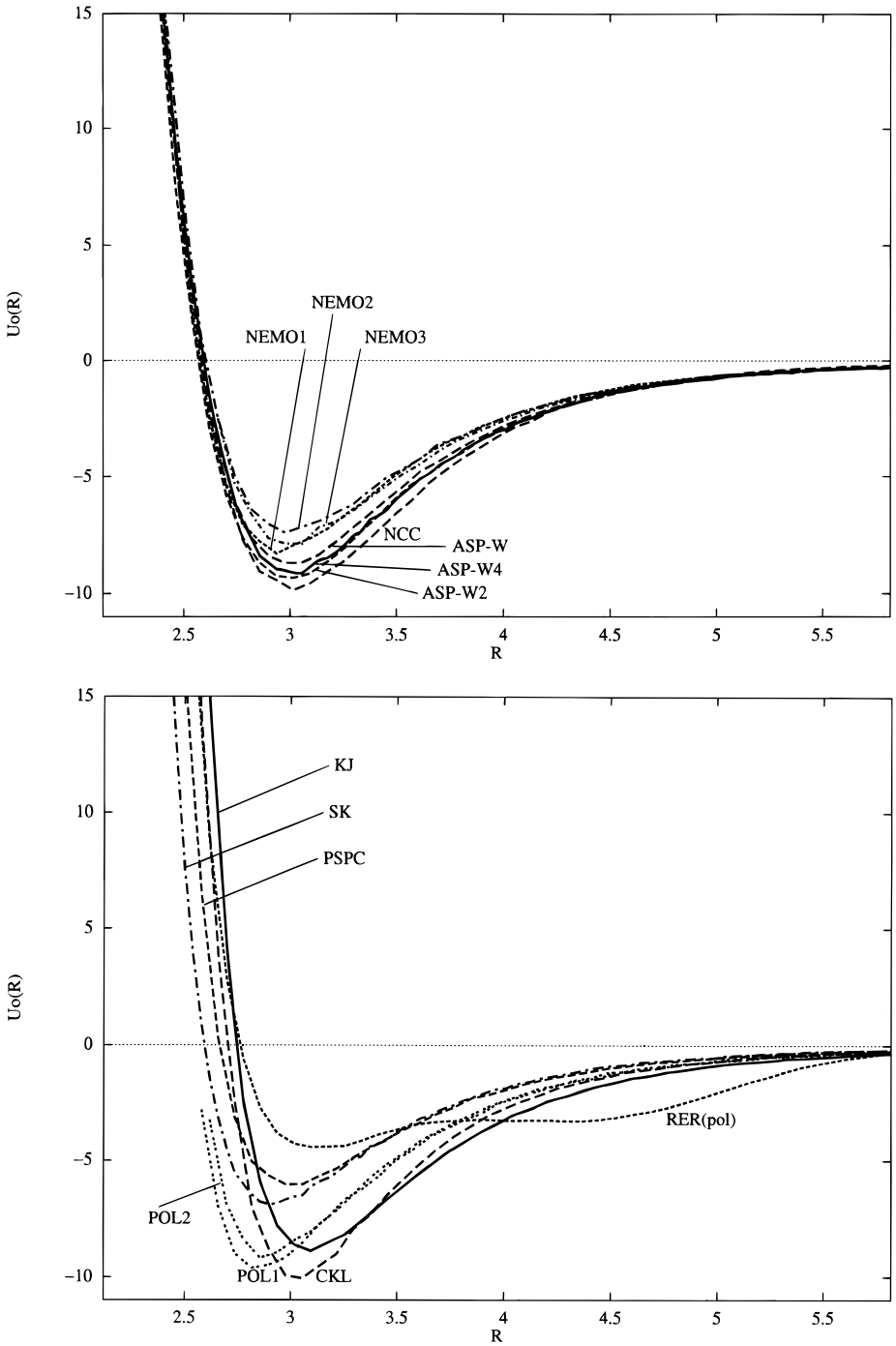

Figure 4. Orientationally averaged pseudopotential $U_0(R)$ (kJ mol^{-1}) (see text for definition) for some polarizable water models vs the center of mass separation R (Å) at 373 K: (a) ASP-W, ASP-W2, ASP-W4, NCC, and NEMO1−3; (b) PSPC, POL1−2, RER(pol), SK, CKL, and KJ.

The calculated results for the second virial coefficient are given in Tables 17−19 and Figure 3. Analysis of subaverages and repetition of some calculations indicate that the error bars on the reported values of $B(T)$ are roughly ±1% in general, but ±3% for values smaller than 50 cm^3 mol^{-1} and up to ± 10−20% for values smaller than 5 cm^3 mol^{-1}. This holds for all the potentials except POL1, POL2, and NEMO3, for which the error bars are roughly twice as large because of the uncertainties in the proper integration of the orientationally averaged Mayer function, as explained in the preceding section.

From these results, we can see that the second virial coefficient is very model-dependent. The simpler nonpolarizable models often differ more substantially from each other, but even the polarizable potentials fitted to ab initio calculations lead to significantly different results. The comparison of the binding energies of the PES global minimum (Table 5) with numerical values of $B(T)$ for each potential clearly shows that it is not possible to correlate these properties unambiguously. $B(T)$ is indeed a global property of the PES, very sensitive to the global minimum region but not exclusively so.

Our results for $B_{cl}(T)$ for ASP-W are obtained from a better sampling than in the original paper.[24] For NCC, we are in exact agreement with the calculation in the literature.[18] For CKL, our results range from 5% less negative than in the original work[17] at 423 K to 6.5% less negative at 673 K; on the other hand, for KJ, our values are roughly 2−3% more negative. We attribute these discrepancies to differences in the sampling.

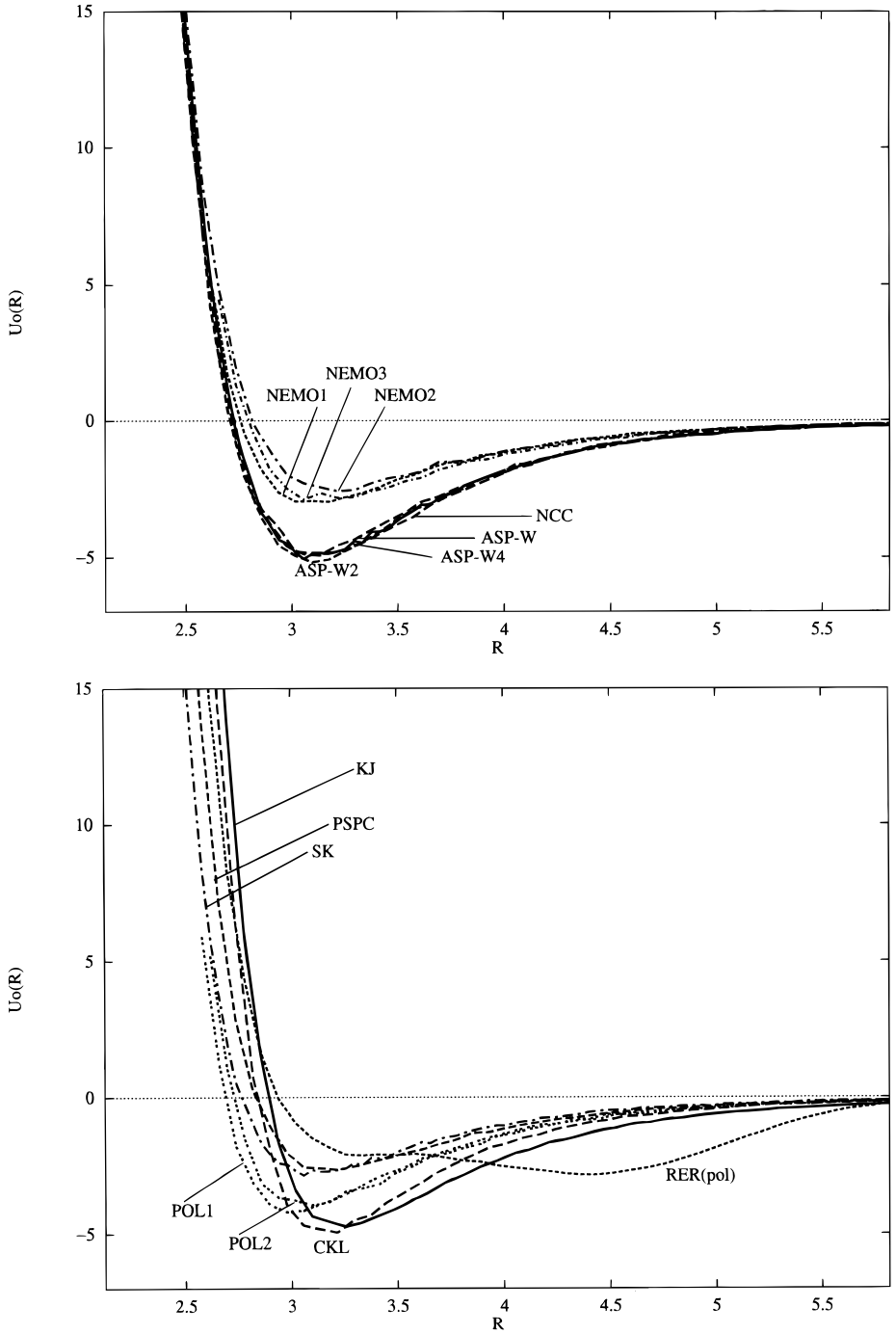

Figure 5. Orientationally averaged pseudopotential $U_0(R)$ (kJ mol^{-1}) (see text for definition) for some polarizable water models vs the center of mass separation R (Å) at 973 K: (a) ASP-W, ASP-W2, ASP-W4, NCC, and NEMO1−3; (b) PSPC, POL1−2, RER(pol), SK, CKL, and KJ.

Computation of the quantum corrections reveals that, between 373 and 973 K, they are in the range 5−15% irrespective of the potential used and that about 90% of the correction arises from the rotational degrees of freedom. These findings are in qualitative agreement with similar calculations by De Santis and Gregori[44] for the TIP4P and MCY potentials and are linked to the small moments of inertia of the water molecule. However, with TIP4P and MCY, the quantum corrections are larger than with the polarizable models (20−25% at 373 K).

When the first-order quantum corrections are included, the best agreement with the most recent experimental values[43] is found for the KJ, ASP, and NCC potentials. Surprisingly, the NEMO potentials, obtained from fitting to high-quality ab initio calculations, give values for $B(T)$ that are not negative enough. The RER(pol) potential, which has the smallest binding energy for the minimum energy dimer (−14.6 kJ mol^{-1}), leads nevertheless to $B(T)$ in reasonable agreement with experiment at the highest temperature. At first sight, this is surprising but it is understood by examination of the orientationally averaged Mayer function $f(R)$ or the orientationally averaged pseudopotential $U_0(R)$ defined by $f(R) = e^{-U_0(R)/kT} - 1$, which is shown in Figures 4 and 5 for the temperatures 373 and 973 K, respectively. In the case of RER(pol), $U_0(R)$ exhibits a second broad minimum near 4.5 Å, contributing to more negative values of $B(T)$ than would otherwise have been expected. The existence of this second minimum can be understood by plotting the energy of particular dimers with respect to the distance R between the centers of mass. This is illustrated in Figure 6,

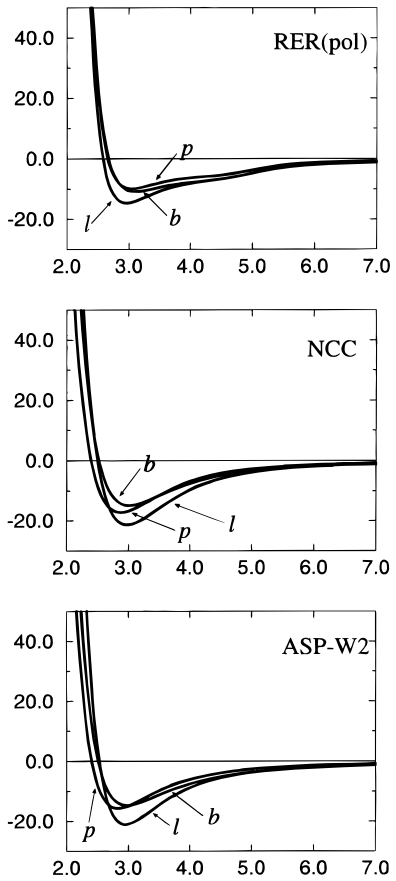

Figure 6. Dimer energy (kJ mol^{-1}) vs center of mass separation R (Å) for the linear (l), planar cyclic (p), and bifurcated (b) dimers for three potentials. Each curve is drawn starting at the stationary point of the potential energy surface and varying the distance R between the centers of mass without changing the orientations of the molecules.

where such curves are given for RER(pol), ASP-W2, and NCC, starting from the geometries of three stationary points (linear, planar cyclic, and bifurcated dimers for each potential). ASP-W2 and NCC have a monotonic R -dependence when R is larger than 3.2 Å, but the energy curves for RER(pol) exhibit an inflexion near 4.8 Å. This behavior is an artifact of RER(pol) and is not shared by the other potentials.

From these calculations, it is possible to delineate some basic features of a water model that are needed to reproduce the second virial coefficient correctly over a wide range of temperatures. As we have already noticed, KJ, ASP-W2, ASP-W4,and NCC all reproduce $B(T)$ satisfactorily. However, $U_0(R)$ for KJ has a repulsive wall at larger R than the other three. In the repulsive wall region, all the potentials coincide approximately, except KJ, CKL, RER(pol), and PSPC (see Figures 4 and 5). The ab initio potentials ASPs, NCC, and NEMOs are expected to be more accurate than the others, so it is likely that the behavior of $U_0(R)$ in the hard wall region predicted by these potentials is the correct one. Two other important features of the $U_0(R)$ curves are the position and energy of the minimum. From Figures 4 and 5 one can observe large discrepancies between the various models. It is particularly clear at 973 K (Figure 5) that POL1, POL2, RER(pol), PSPC, and NEMO potentials are too high in energy at the minimum.

Calculations at 323 K led to $B_{cl} = -921$ cm^3 mol^{-1} and $\Delta B_{qu} = 195$ cm^3 mol^{-1} for ASP-W4; $B_{cl} = -990$ cm^3 mol^{-1} and $\Delta B_{qu} = 224$ cm^3 mol^{-1} for ASP-W2; and $B_{cl} = -1168$ cm^3 mol^{-1} and $\Delta B_{qu} = 270$ cm^3 mol^{-1} for NCC, showing that the first-order quantum corrections amount to some 21−23% of the classical value; this is roughly twice as large as was found with two Stockmayer models of water[45,46] and a modified polarizable Stockmayer model.[47] At 273 K, the experimental value of −1782.8 cm^3 mol^{-1} has been given;[42] we found −1467, −1559, and −1992 cm^3 mol^{-1} for ASP-W4, ASP-W2, and NCC, respectively (with quantum corrections included, representing between 32 and 35% of the classical value). Taking into account that the experimental value is probably slightly too negative (see Table 16), it can be expected that ASP-W4 and ASP-W2 are probably quite accurate down to 273 K.

Recently Mas et al.[88] have developed new potentials for water dimer fitted to symmetry-adapted perturbation theory calculations. Their best potential gives values of $B(T)$ that are very close to the experimental values, with deviations similar in magnitude to those for the ASP-W2 and ASP-W4 potentials. The uncertainty in the experimental values is such that it is not possible to discriminate between their potential and ours on the basis of the virial coefficient.

VI. Conclusions

As we have seen, the calibration of the potential to reproduce the best ab initio calculations on the minimum energy dimer does not ensure that the topology of the potential will be correct. Most of the polarizable potentials tested use a simple functional form and have been empirically parametrized, so they almost certainly lead to an oversimplified potential energy surface. The new ab initio potentials ASP-W4 and ASP-W2 presented in the present work and others from the literature appear to give a more detailed picture of the PES, but none agree exactly with the results of the study of Smith et al. (SSPSR)[30] in the energy ordering of the stationary points and their Hessian indices. Nevertheless, we should bear in mind that the topology of the PES, particularly the Hessian index, is quite sensitive to the basis set used and also that although the ab initio stationary points used as a reference were obtained from high-quality ab initio calculations, they were not corrected for basis set superposition error, and the geometries and energies of the stationary points relative to the minimum energy structure would change if this correction were applied.

It thus appears from this study that the polarizable potentials available can lead to quite different results for the dimer PES and for the pathways for interchange of the hydrogen atoms. Even the potentials calibrated using ab initio calculations are not consistent with each other. Ab initio calculations including correlation are very difficult to carry out accurately. We therefore need other methods to test the quality of potentials.

The new ASP-W2 and ASP-W4 potentials give values of the second virial coefficient $B(T)$ that are close to experiment in the range 373−973K when first-order quantum corrections are included. The quantum corrections are substantial, amounting to 10−15% of the classical value at 373 K, 20−25% at 323 K, and 30−35% at 273 K, and about 90% of the corrections arise from rotational degrees of freedom. The virial coefficient is by no means a complete test of a potential energy surface and in particular has nothing to tell us about many-body effects, but this agreement is encouraging. Other polarizable water potentials from the literature do not perform as well; in fact only one of them is really successful in reproducing $B(T)$, namely, the potential due to Kozack and Jordan,[23] which was fitted specifically to reproduce $B(T)$, although the NCC potential,[18] based on ab initio calculations, is also good in this respect. The recent potential by Mas et al.[88] also performs very well, and in view of the uncertainty in the experimental values it is not possible to discriminate between their potential and ours on the basis of the virial coefficient.

Many more tests are required to check the quality of a potential. For example, it is known from molecular dynamics simulations that the Kozack−Jordan potential does not reproduce the liquid structure correctly at 300 K[23] and that the Niesar−Corongiu−Clementi one gives the wrong pressure.[18] The ASP-W potential has given good results for the tunnelling splittings in the water dimer spectrum,[89,90] but the new potentials have not yet been tested in this way. Spectroscopic results are now available for the small water clusters up to $(H_2O)_6$, and these will provide another valuable test-bed for water potentials, since they will explore the validity of the many-body description. Comparisons between the predictions of the ASP-W2 and ASP-W4 potentials and ab initio calculations for water clusters up to the pentamer show that they are in excellent agreement in general.[91]

We consider that the success of our potentials shows the value of the approach that we have adopted: that is, to work within a perturbation-theory framework, and to use the best available ab initio method to evaluate each contribution to the potential. This approach helps to clarify the limitations in each contribution to the potential and to identify ways of overcoming them.

Acknowledgment. We thank the IDRIS for an allocation of computer time at the CNUSC (Montpellier). We thank Dr. G. Corongiu, Prof. E. Clementi, and Dr. P. O. Åstrand for help with the use of the NCC and NEMO potentials, respectively, and Dr. C. Chipot and Prof. Kollman's group at UCSF for details of the POL1 and POL2 potentials. We thank the EPSRC for financial support for M.P.H. and for provision of computing facilities.

References and Notes

(1) Weber, T. A.; Stillinger, F. H. *J. Phys. Chem.* **1982**, *86*, 1314.
(2) Halley, J. W.; Rustad, J. R.; Rahman, A. *J. Chem. Phys.* **1993**, *98*, 4110.
(3) Bernal, J. D.; Fowler, R. H. *J. Chem. Phys.* **1933**, *1*, 515.
(4) Rowlinson, J. S. *Trans. Faraday Soc.* **1949**, *45*, 974. Rowlinson, J. S. *Trans. Faraday Soc.* **1951**, *47*, 120.
(5) Rahman, A.; Stillinger, F. H. *J. Chem. Phys.* **1971**, *55*, 3336.
(6) Stillinger, F. H.; Rahman, A. *J. Chem. Phys.* **1974**, *60*, 1545.
(7) Berendsen, H. J. C.; Postma, J. P. M.; van Gunsteren, W. F.; Hermans, J. In *Intermolecular Forces*; Pullman, B., Ed.; Reidel: Dordrecht, 1981; p 331.
(8) Jorgensen, W. L. *J. Am. Chem. Soc.* **1981**, *103*, 335. Jorgensen, W. L. *J. Chem. Phys.* **1982**, *77*, 4156. Jorgensen, W. L.; Chandrasekhar, J.; Madura, J. D.; Impey, R. W.; Klein, M. L. *J. Chem. Phys.* **1983**, *79*, 926.
(9) Reimers, J. R.; Watts, R. O.; Klein, M. L. *Chem. Phys.* **1982**, *64*, 95.
(10) Heinzinger, K.; Bopp, P.; Jancsó, G. Acta Chim. Hung. **1986**, *121*, 27.
(11) Wallqvist, A.; Berne, B. J. *J. Phys. Chem.* **1993**, *97*, 13841.
(12) Barnes, P.; Finney, J. L.; Nicholas, J. D.; Quinn, J. E. *Nature* **1979**, *282*, 459.
(13) Rullmann, J. A. C.; van Duijnen, P. T. *Mol. Phys.* **1988**, *63*, 451.
(14) Sprik, M.; Klein, M. L. *J. Chem. Phys.* **1988**, *89*, 7556.
(15) Ahlström, P.; Wallqvist, A.; Engström, S.; Jönsson, B. *Mol. Phys.* **1989**, *68*, 563.
(16) Caldwell, J.; Dang, L. X.; Kollman, P. A. *J. Am. Chem. Soc.* **1990**, *112*, 9144.
(17) Cieplak, P.; Kollman, P. A.; Lybrand, T. *J. Chem. Phys.* **1990**, *92*, 6755.
(18) Niesar, U.; Corongiu, G.; Clementi, E.; Kneller, G. R.; Bhattacharya, D. K. *J. Phys. Chem.* **1990**, *94*, 7949.
(19) Wallqvist, A.; Ahlström, P.; Karlström, G. *J. Phys. Chem.* **1990**, *94*, 1649.
(20) Wallqvist, A. *Chem. Phys.* **1990**, *148*, 439.
(21) Sprik, M. *J. Chem. Phys.* **1991**, *95*, 6762.
(22) Dang, L. X. *J. Chem. Phys.* **1992**, *97*, 2659.
(23) Kozack, R. E.; Jordan, P. C. *J. Chem. Phys.* **1992**, *96*, 3120.
(24) Millot, C.; Stone, A. J. *Mol. Phys.* **1992**, *77*, 439.
(25) Åstrand, P. O.; Wallqvist, A.; Karlström, G. *J. Chem. Phys.* **1994**, *100*, 1262.
(26) Franken, K. A.; Dykstra, C. E. *J. Chem. Phys.* **1994**, *100*, 2865.
(27) Åstrand, P. O.; Linse, P.; Karlström, G. *Chem. Phys.* **1995**, *191*, 195.
(28) Kusalik, P. G.; Liden, F.; Svishchev, I. M. *J. Chem. Phys.* **1995**, *103*, 10169.
(29) Corongiu, G. Int. *J. Quantum. Chem.* **1992**, *42*, 1209.
(30) Smith, B. J.; Swanton, D. J.; Pople, J. A.; Schaefer, H. F., III; Radom, L. *J. Chem. Phys.* **1990**, *92*, 1240.
(31) Saykally, R. J.; Blake, G. A. Science **1993**, *259*, 1570.
(32) Liu, K.; Cruzan, J. D.; Saykally, R. J. *Science* **1996**, *271*, 929.
(33) Wales, D. J. In *Theory of Atomic and Molecular Clusters*; Springer-Verlag: Heidelberg, **1997**; Vol. 2.
(34) Guissani, Y.; Guillot, B. *J. Chem. Phys.* **1993**, *98*, 8221.
(35) Kong, Y. C.; Nicholson, D.; Parsonage, N. G. *Mol. Simul.* **1994**, *13*, 39.
(36) Evans, D. J.; Watts, R. O. *Mol. Phys.* **1974**, *28*, 1233.
(37) Lie, G. C.; Clementi, E. *J. Chem. Phys.* **1976**, *64*, 5308.
(38) Refson, K.; Lie, G. C.; Clementi, E. *J. Chem. Phys.* **1987**, *87*, 3634.
(39) Slanina, Z. *J. Chim. Phys.* **1991**, *88*, 2381. Slanina, Z. *Croat. Chem. Acta* **1991**, *64*, 37. Slanina, Z. *Chem. Phys. Lett.* **1991**, *179*, 355.
(40) Vukalovich, M. P.; Traskhtengerts, M. S.; Spiridonov, G. A. *Teoploenergetika* **1967**, *14*, 65.
(41) Kell, G. S.; Mc Laurin, G. E.; Whalley, E. *J. Chem. Phys.* **1968**, *48*, 3805.
(42) Haar, L.; Gallagher, J. S.; Kell, G. S. *NBS/NRC Steam Tables*; Hemisphere: Washington, DC, 1984.
(43) Kell, G. S.; Mc Laurin, G. E.; Whalley, E. *Proc. R. Soc. Lond.* **1989**, *A425*, 49.
(44) De Santis, A.; Gregori, A. *Chem. Phys. Lett.* **1989**, *160*, 55.
(45) McCarty, Jr., M.; Babu, S. V. K. *J. Phys. Chem.* **1970**, *74*, 1113.
(46) Pompe, A.; Spurling, T. H. Aust. J. Chem. **1973**, *26*, 855.
(47) MacRury, T. B.; Steele, W. A. *J. Chem. Phys.* **1974**, *61*, 3366.
(48) Rijks, W.; Wormer, P. E. S. *J. Chem. Phys.* **1989**, *90*, 6507. See also Erratum: *ibid.* **1990**, **92**, 5754.
(49) Szczęśniak, M. M.; Brenstein, R. J.; Cybulski, S. M.; Scheiner, S. *J. Phys. Chem.* **1990**, *94*, 1781.
(50) Stone, A. J.; Alderton, M. *Mol. Phys.* **1985**, *56*, 1047.
(51) *MOLPRO*: a package of ab initio programs written by H.-J. Werner and P. J. Knowles, with contributions from J. Almlöf, R. D. Amos, M. J. O. Deegan, S. T. Elbert, C. Hampel, W. Meyer, K. Peterson, R. Pitzer, A. J. Stone, P. R. Taylor, and R. Lindh, 1994.
(52) Stone, A. J. *Mol. Phys.* **1978**, *36*, 241.
(53) Wormer, P. E. S.; Hettema, H. *J. Chem. Phys.* **1992**, *97*, 5592.
(54) Stone, A. J. *Chem. Phys. Lett.* **1993**, *211*, 101.
(55) Stone, A. J.; Dullweber, A.; Hodges, M. P.; Popelier, P. L. A.; Wales, D. J. Orient: a program for studying interactions between molecules, version 3.2; University of Cambridge, 1995.
(56) Pohorille, A.; Pratt, L. R.; LaViolette, R. A.; Wilson, M. A.; MacElroy, R. D. *J. Chem. Phys.* **1987**, *87*, 6070.
(57) Wales, D. J.; Ohmine, I. *J. Chem. Phys.* **1993**, *98*, 7257.
(58) Murrell, J. N.; Laidler, K. J. *Trans. Faraday Soc.* **1968**, *64*, 371.
(59) Rybak, S.; Jeziorski, B.; Szalewicz, K. *J. Chem. Phys.* **1991**, *95*, 6576.
(60) van Duijneveldt, J. G. C. M.; van Duijneveldt, F. B. *J. Chem. Phys.* **1992**, *97*, 5019.
(61) Feller, D. *J. Chem. Phys.* **1992**, *96*, 6104.
(62) Xantheas, S. S.; Dunning, T. H. *J. Chem. Phys.* **1993**, *99*, 8774.
(63) Chakravorty, S. J.; Davidson, E. R. *J. Phys. Chem.* **1993**, *97*, 6373.
(64) Wang, Y.-B.; Tao, F.-M.; Pan, Y.-K. J. Mol. Struct. (THEOCHEM) **1994**, 309, 235.
(65) Kim, K. S.; Mhin, B. J.; Choi, U. S.; Lee, K. *J. Chem. Phys.* **1992**, *97*, 6649.
(66) Feyereisen, M. W.; Feller, D.; Dixon, D. A. *J. Phys. Chem.* **1996**, *100*, 2993.
(67) Barnett, R. N.; Landman, U. *Phys. Rev. B* **1993**, *48*, 2081.
(68) Bertran, J.; Ruiz-Lopez, M. F.; Rinaldi, D.; Rivail, J. L. Theor. Chim. Acta **1992**, *84*, 181.
(69) van Hensbergen, B.; Block, R.; Jansen, L. *J. Chem. Phys.* **1982**, *76*, 3161.
(70) Vos, R. J.; Hendriks, R.; van Duijneveldt, F. B. *J. Comput. Chem.* **1990**, *11*, 1.
(71) Muguet, F. F.; Robinson, G. W.; Bassez-Muguet, M.-P. *Int. J. Quantum. Chem.* **1991**, *39*, 449.
(72) Marsden, C. J.; Smith, B. J.; Pople, J. A.; Schaefer, H. F., III; Radom, L. *J. Chem. Phys.* **1991**, *95*, 1825.
(73) Cho, M.; Fleming, G. R.; Saito, S.; Ohmine, I.; Stratt, R. M. *J. Chem. Phys.* **1994**, *100*, 6672.
(74) Sim, F.; St-Amant, A.; Papai, I.; Salahub, D. *J. Am. Chem. Soc.* **1992**, *114*, 4391.
(75) Amos, R. D. *Chem Phys.* **1986**, *104*, 145.

(76) Frisch, M. J.; Del Bene, J. E.; Binkley, J. S.; Schaefer, H. F., III; *J. Chem. Phys.* **1986**, *84*, 2279.
(77) Bentwood, R. M.; Barnes, A. J.; Orville-Thomas, W. J. *J. Mol. Spectrosc.* **1980**, *84*, 391.
(78) Owicki, J. C.; Shipman, L. L.; Scheraga, H. A. *J. Phys. Chem.* **1975**, *79*, 1794.
(79) Hodges, M. P.; Stone, A. J. http://fandango.ch.cam.ac.uk/ 1997.
(80) Bone, R. G. A.; Rowlands, T. W.; Handy, N. C.; Stone, A. J. *Mol. Phys.* **1991**, *72*, 33.
(81) Dyke, T. R. *J. Chem. Phys.* **1977**, *66*, 492.
(82) Coudert, L. H.; Hougen, J. T. *J. Mol. Spectrosc.* **1988**, *130*, 86.
(83) Landau, L. D.; Lifshitz, E. M. *Statistical Physics. Course of Theoretical Physics, Vol. 5*; Pergamon: New York, 1980.
(84) Powles, J. G.; Rickayzen, G. *Mol. Phys.* **1979**, *38*, 1875.
(85) Gray, C. G.; Gubbins, K. E. *Theory of Molecular Fluids. Volume 1: Fundamentals*; Clarendon Press: Oxford, 1984.
(86) Press, W. H.; Teukolsky, S. A.; Vetterling, W. T.; Flannery, B. P. *Numerical Recipes in Fortran*, 2nd ed.; Cambridge University Press: Cambridge, 1992.
(87) Eubank, P. T.; Joffrion, L. L.; Patel, M. R.; Waronwy, W. *J. Chem. Thermodyn.* **1988**, *20*, 1009.
(88) Mas, E. M.; Szalewicz, K.; Bukowski, R.; Jeziorski, B. *J. Chem. Phys.* **1997**, *107*, 4207.
(89) Althorpe, S. C.; Clary, D. C. *J. Chem. Phys.* **1994**, *101*, 3603.
(90) Gregory, J. K.; Clary, D. C. *J. Chem. Phys.* **1995**, *102*, 7817.
(91) Hodges, M. P.; Stone, A. J.; Xantheas, S. S. *J. Phys. Chem.* **1997**, *101*, 9163.
(92) Hill, P. G.; MacMillan, R. D. C. *Ind. Eng. Chem. Res.* **1988**, *27*, 874.
(93) Lide, D. R., ed. *CRC Handbook of Physics and Chemistry*; 75th ed.; CRC Press, Inc.: Boca Raton, 1995.